Design and aerodynamic analysis of side wind deflector for three-wheel vehicle

Getinet Abebayehu Abebe

A Thesis Submitted to the Department of Mechanical Engineering

College of Mechanical, Chemical and Materials Engineering

Presented in Partial Fulfillment of the Requirement for the Degree of Master's in Automotive Engineering

Office of graduate studies

Adama Science and Technology University

January, 2025

Adama, Ethiopia

Design and aerodynamic analysis of side wind deflector for three-wheeler vehicles

Getinet Abebayehu Abebe

Advisor: Dr. Ramesh Babu Nallamothu

A thesis submitted to the Department of Mechanical Engineering,

College of Mechanical, Chemical and Materials Engineering

Presented in Partial Fulfillment of the Requirement for the Degree of Master's in Automotive Engineering

Office of graduate studies

Adama Science and Technology University

January, 2025

Adama, Ethiopia

DECLARATION

I hereby declare that this Master thesis entitled "**Design and aerodynamic analysis of side wind deflector for three-wheel Vehicle"** is my own work and has not been submitted for the award of any academic degree, diploma or certificate in any other university. All sources of materials that are used for this thesis have been duly acknowledged through citation.

____________________	____________________	________________
Name of the student	Signature	Date

RECOMMENDATION

I, the advisor of this thesis, hereby certify that I have read the revised version of the thesis entitled **"Design and aerodynamic analysis of side wind deflector for three-wheel Vehicle"** prepared under my guidance by Getinet Abebayehu submitted in partial fulfillment of the requirements for Master of science in automotive engineering. Therefore, I recommend the submission of the revised version of the thesis to the department following the applicable procedures.

Dr. Ramesh Babu Nallamothu	______________________	______________________
Major Advisor	Signature	Date
______________________	______________________	______________________
Co- Advisor	Signature	Date

APPROVAL

I, the advisor of the thesis entitled **"Design and aerodynamic analysis of side wind deflector for three-wheel vehicle"** and developed by Getinet Abebayehu Abebe; hereby certify that the recommendation and suggestion made by the board of examiners are appropriately incorporated in the final version of the thesis.

Dr. Ramesh Babu Nallamothu	____________________	______________
Major Advisor	Signature	Date

We, the undersigned, members of the Board of examiners of the thesis by Getinet Abebayehu have read and evaluated the thesis entitled **"Design and aerodynamic analysis of side wind deflector for three-wheel Vehicle"** and examined the candidate during open defense. This is, therefore, to certify that the thesis is accepted for partial fulfillment of the requirements for Master of Science in Automotive Engineering.

____________________	____________________	____________________
Chairperson	Signature	Date
____________________	____________________	____________________
Internal examiner	Signature	Date
____________________	____________________	____________________
External examiner	Signature	Date

Final approval and acceptance of the thesis is contingent upon submission of its final copy to the Office of Postgraduate Studies (OPGS) through the Department Graduate Council (DGC) and School Graduate Committee (SGC).

____________________	______________	______________
Department head	Signature	Date
____________________	______________	______________
School Dean	Signature	Date
____________________	______________	______________
Office of Postgraduate Studies, Dean	Signature	Date

TABLE OF CONTENTS

LIST OF FIGURES

LIST OF TABLES

ACRONYMS

ASTU	Adama science and technology university
CAD	Computer aided design
CFD	Computational fluid dynamics

NOMENCLATURE

A	Area (frontal area) m^2
Cd	Drag coefficient (dimensionless)
Cl	Lift coefficient (dimensionless)
D	Drag force (N)
L	Lift force (N)
V	Vehicle speed (m/s)
P	Density of the air (kg/m^3)
q	Dynamic pressure (Pa)
U	Air speed (m/s)

ABSTRACT

Transportation plays a crucial role in our daily lives, and three-wheeled vehicles are an essential part of public transportation. However, many three-wheeled vehicles, particularly Bajaj models, lack side doors, leading to challenges such as passenger discomfort due to wind pressure, increased drag force during motion, reduced vehicle speed, higher fuel consumption, and compromised stability. The primary objective of this thesis is to design and perform an aerodynamic analysis of a side wind deflector for Bajaj three-wheelers to improve passenger comfort and reduce drag force. The methodology begins with a comprehensive literature review to understand the aerodynamic challenges faced by three-wheelers, particularly the impact of drag force on fuel efficiency and stability. Following this, the problems of high drag and wind buffeting are identified, which necessitate the introduction of a wind deflector. A detailed 3D model of the vehicle, based on specific parameters such as wheelbase, frame type, and dimensions, is created using CATIA V5. This model is then analyzed using ANSYS for Computational Fluid Dynamics (CFD) simulations to evaluate the effects of the wind deflector on aerodynamic performance. The study incorporates design optimization using Response Surface Methodology (RSM), examining the impact of deflector angle and width on drag and lift forces. These results demonstrate a significant improvement in aerodynamic performance due to the wind deflector with a 30° angle and 15 cm width. Specifically, there is a **16.8% reduction** in drag force, and a **13.14% reduction** in lift force. These improvements lead to better fuel efficiency, enhanced vehicle stability, and reduced wind noise. The wind deflector also positively impacts airflow behavior and reduces pressure inside the cabin, contributing to enhanced passenger comfort. The findings suggest that the incorporation of a wind deflector with a 30° angle and 15 cm width can substantially improve both the aerodynamic performance and overall comfort of Bajaj three-wheelers.

Keywords: Aerodynamic, ANSYS, CAD model, CATIA, drag force.

CHAPTER ONE

INTRODUCTION

1.1 Background of the Study

A three-wheeler is a vehicle with three wheels, most commonly one wheel at the front and two at the rear. Most three-wheeler vehicles use the engine on the rear side. Three-wheelers are known by many terms in various countries, including auto, rickshaw, baby taxi, moto taxi, pigeon, Jonny bee, Bajaj, Chand gari, Lapa, tuktuk, tum-tum, keke-napep, Marwa, 3-wheel, bao-bao, easy bike, CNG, and tucuxi (Auto rickshaw Wikipedia, 2023). Three-wheeler RE Bajaj is shown in Figure 1.1.

Figure 1.1: Three-wheeler RE Bajaj

The most common type is characterized by a sheet-metal body or open frame resting on three wheels, a canvas roof with a drop-down side curtain, a small cabin at the front for the driver and operating handlebar controls, and three passenger seats at the back side. They are especially common in countries with tropical or subtropical climates since they are usually not fully enclosed, and they are found in developing countries because they are relatively inexpensive to own or operate (encyclopedia-auto rickshaw2023).

Bajaj Auto is an Indian multinational automotive manufacturing company based in Pune. It was founded by Jamnalal Bajaj (1889–1942) in Rajasthan in the 1940s. This company is the world's largest three-wheeler manufacturer (Dhurve,2023).

The Bajaj RE three-wheeler has become a vital component of the informal transportation sector in numerous countries, especially in regions with high population density and limited public transport infrastructure. In cities and rural areas alike, Bajaj three-wheelers are used to ferry passengers and deliver goods across narrow and congested streets, where traditional cars and larger vehicles are not always practical. These vehicles are especially popular in countries such as India, Nigeria, Bangladesh, Thailand, and Ethiopia, due to their low acquisition and operating costs.

In Ethiopia, Bajaj three-wheelers are commonly referred to as Bajaj. They play a crucial role in the country's transportation system, providing an affordable means of travel for the urban and rural population. The widespread use of Bajaj three-wheelers in Ethiopia reflects their importance as a low-cost solution for short-distance travel, especially in areas where buses and taxis may be less accessible or too expensive. These vehicles also offer significant flexibility, enabling drivers to easily navigate crowded streets and reach remote areas where larger vehicles may struggle.

The Bajaj RE is widely regarded for its fuel efficiency, compact design, and reliability, which make it suitable for navigating the challenging and often poor road conditions that characterize many parts of developing countries. The vehicle's open cabin and simple structure allow for easy maintenance, making it an attractive option for owners and drivers who may not have access to advanced tools or expensive service centers. This durability and practicality have made the Bajaj RE a popular choice for both daily transportation and small-scale cargo delivery.

Bajaj Auto's contribution to the global three-wheeler market has been immense, with its vehicles reaching various international markets. The company's innovation in designing three-wheelers that cater to the needs of both drivers and passengers has helped to elevate the role of these vehicles in the transportation networks of numerous countries. Bajaj's commitment to sustainable mobility has also led to the development of eco-friendly three-wheelers that run on compressed natural gas (CNG) or electricity, addressing environmental concerns while providing a cost-effective transport solution.

Despite the widespread adoption of Bajaj three-wheelers, challenges still exist regarding their performance, particularly in terms of comfort and aerodynamic efficiency. In areas with high wind speeds, passengers in open three-wheelers can experience discomfort due to wind pressure and drag, which can reduce the overall stability of the vehicle. However, despite these challenges, Bajaj three-wheelers continue to be an integral part of transportation systems worldwide.

1.2 Statement of the problem

Nowadays, three-wheel bicycles have become the main means of transportation, mostly in undeveloped countries. If we take Ethiopia as an example, the data from the Ethiopian Ministry of Transportation indicates that as of the last fiscal year, 2017, there were more than 200,000 legally registered and unlicensed three-wheel Bajaj's in Ethiopia. Several experts estimate the total number of Bajaj's in Ethiopia in 2022 to be around one million. It would be safe to assume that a single Bajaj can serve at least four people, and therefore we can say that the Bajaj industry directly supports four million Ethiopians (thereporterethiopia.com/31084/).

From the total number of three-wheel Bajaj's, most of them have no driver or passenger doors on the right side. The reason for using the open door on the right side may differ from place to place or person to person. But mostly in the hottest environmental conditions, the right-side door is not preferable due to the compactness of the cabinet and the absence of the air conditioning systems in the three-wheel Bajaj's. Some three-wheel Bajaj drivers prefer to use them without a right-side door for the fastest public transportation systems (to load and unload passengers).

Even if most drivers prefer to use vehicles without right-side doors, there is one problem that arises due to the absence of the right-side door: the wind pressure effect on both the driver and passenger. Also, as the three-wheel Bajaj's is covered with hoods on all the upper and rear sides and the right side remains open, the wind force during the driving will enter the cabinet, and as the speed of the vehicle increases, the drag force due to the entering wind will increase. Due to the increase in drag force, the Bajaj's speed will be limited, and fuel consumption will also increase.

Generally, due to the absence of the right-side door, the three-wheel Bajaj will encounter the following problems:

- Uncomfortable transportation for the passengers and driver due to the wind pressure effect.
- Uneven vehicle stability
- Reduction in vehicle speed due to increase in drag force
- Increase in fuel consumption
- Increase in wind buffeting noise

Therefore, to overcome or minimize the above-listed problems, a side door wind deflector is designed for the three-wheel Bajaj. This thesis work deals with the design and aerodynamic analysis of a side wind deflector for the three-wheel Bajaj.

1.3 Objectives

1.3.1 General objective

The general objective of this thesis work is to design and conduct an aerodynamic analysis of a three-wheel Bajaj side wind deflector to reduce the wind pressure effect on the driver and passengers and to reduce the drag.

1.3.2 Specific Objectives

- Design and create a 3D model of a wind deflector for the right side of a three-wheel Bajaj.
- Conduct aerodynamic analysis of the wind deflector model at a speed of 60 km/h.
- Compare the drag force with and without the wind deflector.
- Optimize the dimensions of the 3D model for improved performance.

1.4 Scope of the Study

This research focuses on the design and aerodynamic analysis of a side wind deflector for a three-wheeled Bajaj vehicle. The main objectives include:

- **Designing and Modeling**: Creating a detailed CAD model of the wind deflector specifically for the right side of the Bajaj vehicle, using CATIA software.
- **Aerodynamic Analysis**: Performing an aerodynamic evaluation to assess the effects of the wind deflector on reducing wind pressure and drag force at a constant speed of 60 km/h using ANSYS software.

- **Performance Comparison**: Evaluating the performance of the Bajaj vehicle by comparing drag forces with and without the side wind deflector in place.
- **Optimization**: Iteratively optimizing the design and dimensions of the wind deflector to achieve maximum aerodynamic efficiency.

1.5 Limitation of the study and solutions followed to overcome limitation.

1.5.1 limitation

- **Limited Computational Resources**: The study faced significant constraints due to the lack of access to high-performance computers. The available computing hardware was not optimized for handling resource-intensive simulations, which is critical for accurate aerodynamic analysis. As a result, the processing speed and efficiency were impacted, leading to extended simulation times. This limitation reduced the overall throughput of the analysis and restricted the ability to run a larger number of simulations within the timeframe of the study. Complex simulations that could have provided deeper insights into the aerodynamic behavior of the wind deflector were often constrained by the processing capabilities of the available hardware.
- **Extended Processing Time for Simulations**: The use of **ANSYS** software, while highly effective for aerodynamic analysis, posed its own set of challenges. The simulations required significant processing power, especially when evaluating detailed fluid dynamics around the vehicle with the wind deflector. As a result, each simulation took longer to complete than initially anticipated. This not only delayed the analysis but also limited the number of simulations that could be conducted within the scope of the study. The need for longer processing times made it difficult to perform extensive testing on various design configurations or conduct multiple iterations to refine the model for optimal aerodynamic performance.
- **Impact on Accuracy and Depth of Analysis**: The computational limitations and extended simulation times may have compromised the depth and accuracy of the analysis. The inability to perform a large number of simulations with varied parameters or to iterate on the design model in a timely manner potentially limited the ability to capture the full scope of aerodynamic effects and optimize the deflector design. Ideally, more simulations could have provided a better understanding of how different design

adjustments impact drag reduction and wind pressure mitigation, allowing for a more precise optimization process.

- **Limited Iterative Improvements**: The study's scope was also impacted by the lack of time and resources to conduct iterative improvements on the 3D model based on initial findings. With longer processing times and limited computational power, the research was not able to fully explore all potential design iterations. Consequently, the study's ability to refine the wind deflector model was restricted, meaning that the final design was based on fewer iterations than would have been ideal for maximizing aerodynamic efficiency.
- **Constraints on Testing Conditions**: Due to the processing time limitations, the study could only test the wind deflector model at a single speed (60 km/h), rather than testing over a broader range of velocities. This limited the ability to assess the deflector's performance under varying operational conditions, which would have been important for determining its effectiveness in real-world scenarios. Without the flexibility to test multiple speeds, the overall validity of the study's results is somewhat constrained.

1.5.2 Solutions for Overcoming Limitations:

1.solution for Limited Computational Resources

- Access Higher-Performance Hardware: securing access to high-performance computing resources, can significantly enhance processing speeds and allow for the completion of more complex simulations.
- Use Distributed Computing: systems where multiple machines work together to process simulations more efficiently. Many universities and institutions offer access to such systems for academic purposes.
- Software Optimization: Optimize the simulation settings to strike a balance between accuracy and computational cost. Simplifying the mesh or using approximations in less critical areas of the model may help to reduce simulation time without sacrificing too much accuracy.

2. solution for Extended Processing Time for Simulations

- Parallel Computing: Utilize parallel computing capabilities to divide the task of simulation into smaller chunks that can be processed simultaneously. Many modern simulation software tools, including ANSYS, support this feature.
- Simplify Simulation Complexity: In scenarios where simulations are taking too long, simplifying the model or focusing on key areas of interest rather than running highly detailed simulations for the entire model might help.

3. solution for Impact on Accuracy and Depth of Analysis

- Conduct More Iterative Testing: With access to better computational resources and more processing time, it would be beneficial to conduct multiple iterative simulations to refine the design and improve the accuracy of results. This can be achieved by adjusting parameters (such as the shape or angle of the wind deflector) based on initial findings and running additional simulations.

4. solution for Limited Iterative Model Refinement

- Use Design of Experiments (DOE): Implement a Design of Experiments (DOE) methodology to systematically explore a range of design variables. DOE allows for a structured approach to optimizing the design with fewer iterations while covering a wide range of potential outcomes.

5. solution for Limited Testing Conditions

- Include Environmental Factors: Integrate real-world environmental variables into the simulations, such as wind direction, temperature, and road incline, to make the results more applicable to real-world scenarios.

1.6 Significance of the Study

This study is significant as it addresses multiple aspects of the three-wheeled Bajaj vehicle's performance, safety, comfort, and efficiency. By designing and analyzing the side wind deflector, the research has the potential to bring tangible improvements in the following areas:

1. Creating a Comfortable Means of Transportation for Both Driver and Passengers

- One of the primary goals of this study is to enhance the comfort of both the driver and passengers. Vehicles, especially three-wheelers, are often subjected to high wind resistance during movement, which can create discomfort due to wind pressure and turbulence around the vehicle. The introduction of a side wind deflector mitigates the direct impact of wind hitting the vehicle's side, making the ride smoother and more comfortable. By reducing the wind pressure, passengers will feel less physical strain from gusts of wind, leading to a more enjoyable travel experience. This is particularly important in three-wheelers, where the driver and passengers are often more exposed to the elements compared to traditional enclosed vehicles.

2. Reducing Wind Buffeting Noise

- Wind buffeting noise is a common issue in open or semi-open vehicles, especially in three-wheeled models where the driver and passengers are more exposed to the air. The turbulence caused by the air hitting the vehicle at high speeds can lead to an increase in noise, making the travel experience unpleasant. By using a wind deflector, the vehicle can be shielded from some of this wind turbulence, leading to a reduction in the buffeting noise. The deflector helps redirect the airflow smoothly around the vehicle, thus minimizing the vibration and noise that would otherwise be generated by turbulent air. This results in a quieter ride, which is especially beneficial for long-distance travel, reducing driver fatigue and making the ride more pleasant for passengers.

3. Improving the Stability of the Three-Wheel Bajaj

- The wind deflector plays an essential role in enhancing the stability of the vehicle, particularly in adverse weather conditions or when driving at higher speeds. Crosswinds or gusts of wind can cause instability in vehicles that are lighter or less aerodynamically optimized, such as the three-wheeled Bajaj. By reducing the effects of these external wind forces, the wind deflector ensures the vehicle maintains better control, preventing it from swaying or tipping over. This is especially crucial for safety, as it lowers the risk of accidents due to wind-induced instability. With the added key benefits of improving a vehicle's aerodynamics is the reduction in drag force. When a vehicle moves through the air, it faces resistance due to air molecules colliding with the vehicle's surfaces, which results in drag. For the three-wheeled Bajaj, a high drag force means that the engine has to work harder to overcome the air resistance, leading to increased fuel consumption. By introducing the wind deflector, the aerodynamic properties of the vehicle are optimized, reducing the drag. This allows the vehicle to move more efficiently through the air, requiring less energy (and therefore less fuel) to maintain the same speed. As a result, the vehicle's fuel consumption decreases, which is beneficial for the environment by reducing emissions and for the operator in terms of operating costs. This improvement in fuel efficiency helps make the Bajaj more economical in the long run, leading to savings on fuel and reducing its carbon footprint.

1.7 Organization of the thesis

This thesis is organized into six chapters. Chapter one is an introduction that comprises the background of the study, statement of the problem, objectives and scopes, significance of the study, and organization of the study. Chapter two presents a review of the study of three-wheel Bajaj's. Chapter three presents material and methods. Chapter four presents modeling and aerodynamic analysis for RE4S Bajaj. Chapter five deals with the results and discussion of the analysis. Finally, chapter six deals with the conclusion and recommendation of the thesis.

CHAPTER TWO

LITERATURE REVIEW

2.1 Introduction

This chapter includes vehicle aerodynamics, including the history of vehicle aerodynamics, the need for automotive aerodynamics, aerodynamic forces, and other related topics.

2.2 History of Vehicle Aerodynamics

First, early automotive designers borrowed the shape of the automobile from the shape of ships and airplanes, but this was a wrong approach because ship and airplane body design is taken from the shape of birds and fish. Secondly, vehicle aerodynamics is not considered one of the design parameters for designing the shape of the vehicle body. There was low engine power and bad roads due to this driver's moderate driving speed. This was a problem because the first automobiles were probably slow, and the traditional design of horse-drawn carriages could protect drivers and passengers from wind, mud, and rain. Through time, automobile designers started to find another shape of automobiles away from the improper design (Bappa, 2015).

In the period of 1900–1920, when automobiles started, they also copied the shape of the vehicles from ships and planes. The engineers ignored the ground effect and the loss of symmetry in the flow. Due to the ignorance of the ground effect and the symmetry of the flow, it resulted in an increase in drag force on the vehicles. The engineers also ignored the fact that wheels being out of the chassis of the car make the flow distorted (Gonzalez Casal, 2013). The first prototype car is shown in Figure 2.1.

Figure 2.1: First prototypes of cars based on plans and ships form (Jamais Contente,Alfa Romeof 1914)

In the period of 1920–1970, the first wind tunnel appeared to improve the aerodynamics of automobiles. But the first wind tunnel is not designed to determine the aerodynamic forces of the vehicles; the objective was to determine the forms of the vehicles, which helps reduce the power needed to move the car at certain speeds. Therefore, Paul Jaray was considered the first engineer to design a vehicle's body, keeping in mind the aerodynamics of the vehicle. But at that time, his design was not accepted by consumers. However, over time, the vehicle designer starts to use his idea (Gonzalez Casal, 2013).

Nowadays, the efficiency of vehicles is considered the main design factor in people’s minds. Due to this, it is impossible to design a new car without considering the aerodynamic effect of the vehicle's body. In 2013, Mercedes-Benz CLA announced the most aerodynamic production car with a drag coefficient (CD) of 0.23. To get a minimum number of CDs, it is important to design a vehicle's front, rear, top, and side bodies with the best aerodynamic shape. Mercedes-Benz CLA is shown in Figure 2.2.

Figure 2.2: Mercedes-Benz CLA, whose CD is 0.23 (Gonzalez Casal, 2013)

Recently, Lightyear, the high-tech company developing the world’s first solar car, announced production of vehicles with a minimum (record-breaking) drag coefficient of 0.175 (CD). The lower the drag coefficient, the better the car will efficiently use its energy, giving drivers more range and less reliance on electrical charging Lightyear 2022).

The Lightyear 0 body shape is designed with minimum air resistance; due to this, they achieve a very low drag coefficient. They also keep in mind the vehicle's balance and lift force to ensure a smooth ride. A vehicle with a minimum drag’s coefficient consumes less energy, which helps to drive long distances with a single charge. Due to the reduction of the drag coefficient, Lightyear 0 has become a market frontrunner. Lightyear 0 with 0.175 (Cd) is shown in Figure 2.3.

.

Figure 2.3: Lightyear 0 with 0.175 (Cd) (light year 2022)

2.3 **The Need for Automotive Aerodynamics**

Vehicle aerodynamics can be labeled as the study of fluid dynamics because it deals with air flows through and around the vehicle body, and air is a very thin type of fluid. When the vehicle is driven at high speed, the airflow through and around it begins to have a greater effect on acceleration, top speed, fuel efficiency, and handling.

The importance of improving the flow characteristics

- ✓ to reduce fuel consumption.
- ✓ favorable comfort characteristics (mud deposition on the body, noise, ventilating, and cooling of the passenger compartment).
- ✓ improvement of driving characteristics, stability, handling, and traffic.

2.4 vehicle side wind deflector

Vehicle side door wind deflector is shown in Figure 2.4.

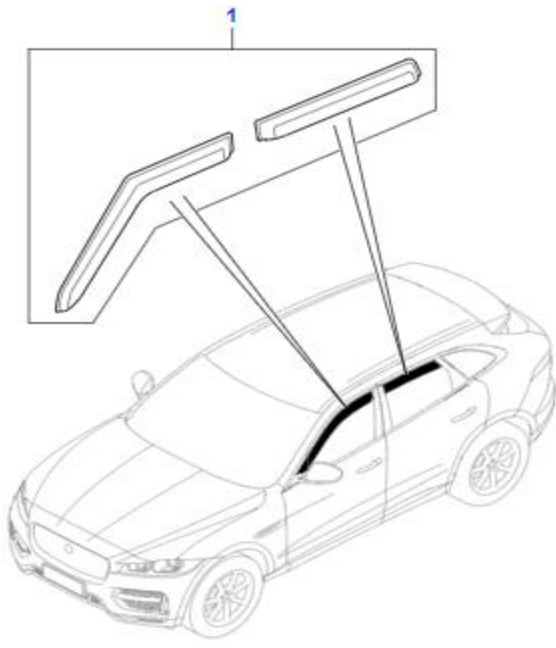

Figure 2.4: Vehicle side wind deflector

Wind deflectors are a useful but usually unnoticed or forgotten car accessory. Wind deflectors, when fitted, channel both air and airborne substances away from the window and down the side of the car (Davis, 2017).

They function based on the idea that an open window disrupts a vehicle's aerodynamics, causing fast-moving air to flow into the car. This leads to stronger winds constantly hitting both the driver and passengers, as well as a significant increase in road noise. Wind deflectors address these issues by subtly modifying the vehicle's aerodynamic shape. When wind strikes the deflectors, it is redirected over the open windows and around the vehicle, preventing it from entering the cabin. Proper ventilation in your van also reduces the need for air conditioning, which can lower fuel consumption.

The Benefits of Wind Deflectors

The deployment of wind deflectors emerges as a pragmatic strategy to mitigate aerodynamic drag in vehicles (Hariram et al., 2021).

- Reducing wind and noise
- Tinted to reduce glare

- Aerodynamic design reduces drag.
- Smooth, slimline design
- Easy to fit
- Supplied in pairs
- Car wash friendly

2.4 Scope of Vehicle Aerodynamics

The flow processes to which a moving vehicle is subject fall into 3 categories:

1. Flow of air around the vehicle.
2. Flow of air through the vehicle's body.
3. Flow processes within the vehicle's machinery (Schuetz, 2015).

2.5 Aerodynamic Forces and Moments

Lift, drag, and side force are the forces that operate along three perpendicular axes. The drag and lift characteristics of a vehicle are crucial factors in its aerodynamics (Hoque, A). Aerodynamic drag is the force that resists the vehicle's motion in the forward direction. Lift forces, on the other hand, push the vehicle either upwards or downwards. Side force arises due to crosswinds or when a vehicle is closely positioned to another. The lift, drag, and pitching moments quantify the tendency of aerodynamic forces to cause rotation around the center of gravity. In crosswind conditions, the side force acts ahead of the center of gravity, causing the vehicle to steer away from the wind and producing a noticeable moment effect (Bappa, M. 2015).

2.5.1 Aerodynamic Drag

Aerodynamic drag is the force that resists the vehicle's movement in the direction of travel. The primary factors contributing to vehicle drag include the high pressure exerted on the front of the vehicle, friction between the vehicle's surface and the air, and the relatively low pressure created behind the vehicle (Moffat, 2016).

The aerodynamic drag force exerted on a vehicle is the combined effect of air resistance encountered as the vehicle moves through the atmosphere (Nath et al., 2021).

Aerodynamic drag is the largest and most important aerodynamic force experienced by road vehicles in motion (Gillespie et al., 1999). It is the force opposite to the direction of motion that acts on a body moving through air (Buscariolo et al., 2016). The friction of air as it approaches the vehicle bodywork is defined as drag. The drag will increase on a vehicle bodywork if more surface area is exposed to the rushing air. An instance could be drawn from the aerodynamic shape of the Volkswagen XL1, which is the most aerodynamic car with a drag coefficient of 0.19. This means that its good aerodynamic shape helps it pass through air more easily than other cars (Bappa, 2015). Reducing drag is important because it saves fuel. The amount of drag force experienced by a road vehicle depends on its shape, size, and airflow (SEIFFERT, 2005). In addition, the amount of drag a vehicle experience is dependent on how aerodynamic it is. A vehicle is considered aerodynamic if the shape of the outside bodywork can reduce drag, which in turn saves fuel.

The drag (D) of a vehicle is influenced by its frontal area (A) and shape, with the aerodynamic quality of the shape represented by the drag coefficient (Cd). Typically, the vehicle's size and frontal area are determined by design requirements, while efforts to reduce drag focus on lowering the drag coefficient. The pressure difference between the vehicle's upper and lower surfaces generates a force perpendicular to the direction of motion, known as lift. Generally, lift acts upwards, tending to raise the vehicle and reduce the effective wheel loads. It is also associated with a pitching moment, which affects the wheel loads at the front and rear differently (Bappa, 2015).

Aerodynamic drag force:

$$D = 0.5\ \rho V^2 \mathrm{ACd} \quad \text{.......... (1)}$$

While drag coefficient, Cd, can be expressed as

$$Cd = D/0.5\rho V^2 \mathrm{A} \quad \text{.......... (2)}$$

Where:

A = frontal area

ρ = density of the air

V = speed of the vehicle relative to the air

Cd = drag coefficient

2.5.2 Aerodynamic drag and Fuel consumption

The rapidly increasing fuel prices and the regulation of greenhouse gases to control global warming give tremendous pressure on design engineers to enhance the current designs of the vehicle using the concepts of aerodynamics to enhance the efficiency of vehicles (Krishnan, P. N. 2009). To improve the fuel consumption, it is necessary to control flow separation at the rear of vehicles by applying flow control mechanisms that help either to delay or prevent the separation effect (Mukut, 2019).

The automobile industry is focused on producing aerodynamically efficient vehicles that not only reduce emissions but also improve fuel economy. Studies have shown that aerodynamic drag increases with the square of the vehicle's speed, with 70% of this drag coming from overall vehicle resistance at high speeds (Lee, S.W. 2018). At highway speeds, overcoming aerodynamic drag accounts for more than 50% of fuel consumption (Bettes, W. 1982).

The prediction of the relationship between fuel consumption and aerodynamic drag is reasonably difficult. This is because the quantity of fuel a vehicle consumes depends on several factors, which include engine efficiency, transmission system, and the power to resist motion. The required power is the product of total resistance force and vehicle speed. It can be rewritten mathematically as power = total resistance force × speed.

The total resistance at a steady speed is the sum of aerodynamic drag and tire rolling resistance. A typical medium-sized European car would be used as an example to show that reducing drag can improve the fuel economy of cars. This car, with a 1.5-liter engine and a drag coefficient of 0.35, uses 7.1 liters per 100 km while driving at a constant speed of 75 mph. Furthermore, with the same vehicle data, there would be a significant decrease in aerodynamic drag by 125 N if the drag coefficient could be decreased to 0.25 and, in turn, reduce the total resistance (rolling and aerodynamic) by 23 percent from 560 N to 432 N at 120 km/h.

The main cause of vehicle aerodynamic drag is due to pressure drag or form drag. Pressure drags on vehicles due to flow separation constitutes more than 80% of the total aerodynamic drag (Wood, R.M. 2004).

Aerodynamic drag is a significant challenge when accelerating a solid body moving through the air. As a racing car or road vehicle burns fuel to accelerate, the drag force acts from behind, reducing speed and negatively impacting fuel efficiency (Hassan, S. 2014). A study on the aerodynamic analysis of cabriolet passenger cars examines a modified cabriolet and compares its performance with that of a closed-roof production vehicle. The flow patterns and the flow velocities, both inside and outside the vehicle, are studied using a commercial computational fluid dynamics (CFD) solver. The result shows that the Cabriolet vehicle drag coefficient is about 32% higher than the closed-roof production vehicle (Regin A et al., 2013).

2.5.3 Aerodynamic Lift

The pressure difference between the top and bottom of a vehicle generates a lift force, which plays a crucial role in driving stability. This lift force is measured at the vehicle's centerline, specifically at the center of the wheelbase (Gillespie et al., 1999). While lift is not a significant concern at normal speeds, it can impact the stability and braking performance of a road car at very high speeds. Lift, in general, opposes the weight of an object. This, in turn, raises it into the air and keeps it there, i.e., an airplane. Meanwhile, downforce is the force that presses an object in the direction of the ground, i.e., a car. Therefore, with the aforementioned definitions, downforce is the opposite of lift force. Furthermore, the generation of lift by road vehicles is to resist or oppose the weight of the car. If the weight of the car is greater than the lift, this results in forward motion, unlike in airplanes, where the lift force is greater than the weight to allow flight (Bappa, 2015).

The lift coefficient is defined as $\mathbf{C_l = L/q\ S}$, where L is the lift force, S is the area of the wing, and q = ($rU^2/2$) is the dynamic pressure with r being the air density and U the airspeed. Similarly, the drag coefficient is written as $\mathbf{C_d = D/q\ S}$, where D is the drag force and the other symbols have the same meaning.

While lift force is quantified by the equation:

$$L = 0.5\ \rho V^2 \mathrm{ACl} \quad (3)$$

where Cl = lift coefficient, A = frontal area ($m^{2)}$, ρ = density of the air (kg/m^3, and V = speed of the vehicle relative to the air (m/s),

2.5.4 Drag Force on Vehicle with and without Deflector

This paper deals with the analysis and calculation of drag force on a vehicle with and without a wind deflector. The model chosen here is a truck; it is modeled in the ANSYS workbench designer module. The vehicle speed is 100 vehicle km/hr., and the results obtained show that the total drag coefficient for vehicles without a wind deflector is 0.98, and the total drag coefficient for vehicles with a wind deflector is 0.85. Therefore, we can simply understand the effect of wind deflectors in the reduction of drag force, which helps us to improve the efficiency and fuel reduction of the vehicle (Reddy et al., 2022).

2.6 Wind buffeting (wind noise)

Wind noise is one of the main noise sources that affect occupant comfort (Wang.Q.2021).

This paper deals with the effect of the rain visor on the reduction of the window buffeting noise. For the numerical simulation, a sedan-type vehicle is selected. For the simplification and reduction of the calculation, the effect of external flow fields like screen wipers, door handles, and other accessories is ignored. The analysis results indicate that installing a visor on the left and right front windows alters the vortex trajectory on both sides, reducing the amount of vorticity that enters the cabin (Yang et al., 2022). Buffeting noise typically occurs when driving a vehicle with a sunroof or rear window open, as shown in a 2007 study by Larry Deaton, Mohan Rao, and Shih Wei-Zen. However, in some cases, it can also happen with the front window open. Buffeting noise is a low-frequency, pulsating sound generated inside the vehicle when driving with a side window open. This noise, which is beyond the human hearing threshold, is perceived by occupants as a pulsation or pressure, particularly on the eardrums. The high sound pressure level of this noise can be so bothersome that prolonged exposure leads to significant fatigue (Deaton et al., 2007).

This paper examines the impact of buffeting noise in passenger cars under real-life conditions at varying speeds. When the rear window is opened 25%, buffeting noise is not noticeable. It becomes perceptible when the window is 50% open, with a resonance frequency of 15.6 Hz at 80 km/h, but the noise is not bothersome due to the low-pressure level (110.2 dB). When the window is 75% open, two airflows form inside the car: one from the upper interior zone and another from the central interior zone. At this point, the buffeting noise becomes clearly noticeable, with a resonance frequency of 16.4 Hz at 80 km/h and a pressure level of 119 db. The frequency increases to 19.5

Hz at 110 km/h, with the pressure level rising to 122 db. Above speeds of 130-140 km/h, the buffeting noise diminishes, depending on the vehicle model (Dunai et al., 2015).

At high speeds, wind noise, also known as buffeting noise, becomes one of the primary sources of noise, particularly when the windows are open for demisting or ventilation (Deaton et al., 2007). This wind buffeting noise, characterized by low frequency and high intensity, can cause fatigue and irritation in passengers, negatively impacting the vehicle's ride comfort and safety (Wang et al., 2017). The wind buffeting noise of a vehicle consists of a quasi-stationary broadband signal, fluctuations caused by aerodynamic turbulence, irregularities of the airflow, cavity resonances, aspiration leaks, and low-frequency beating noise caused by open windows, sunroofs, and gusts of wind (Lemaitre et al., 2015). Due to its complex formation and high intensity, the wind noise generated by vehicle windows has garnered significant attention and is frequently discussed. Previous research has indicated that the wind noise from the vehicle's rear windows tends to be higher than that from the front windows. To enhance ride comfort, reducing the buffeting noise from the rear window has been a primary focus in the field of vehicle noise control engineering over the past few decades (Wang et al., 2017).

2.7 CFD Analysis

Computational Fluid Dynamics (CFD) is a subset of fluid mechanics that employs numerical methods and algorithms to solve and analyze problems involving fluid flow. Computers are utilized to carry out the calculations necessary to simulate how liquids and gases interact with surfaces defined by specific boundary conditions (Satyanarayana, G. 2013). The application of CFD simulations confers a strategic advantage by enabling the virtual testing of diverse wind deflector configurations and other design variations on vehicles (Ariyansah, R. 2019).

CFD represents a numerical approach widely employed for modeling and analyzing fluid flow around objects with intricate geometries, obviating the need for costly and intricate physical testing (Gamayel, A. 2021). The underlying theory of CFD finds its roots in the Navier-Stokes equations, a set of partial differential equations formulated to model fluid behavior (Li et al., 2023).

2.8 Response Surface Methodology and Design Expert

Design of Expert (DE) minimizes the human effort required for optimization by generating multiple design points based on the number of design parameters involved. These design points are created using random values within the specified range for each design parameter, and each case is solved accordingly. Design points can be manually selected, or more commonly, commercial software tools are now available that automatically generate these points according to the problem's requirements. This significantly reduces the need for repetitive tasks, such as altering geometry, re-meshing, and re-inputting solver settings. For this process, software-generated design points have been utilized. Additionally, Response Surface Methodology (RSM) is easily applied to optimization problems that involve multiple disciplines, objectives, and constraints. RSM is a similar process to a curve fitting process. Using the solutions obtained for several design points, a surface approximation is being applied to develop the response surface. By analyzing the regression fit and plotting the response surface and contour lines, the response values for the corresponding output variables can be determined for any given value of the design parameters (Yadav, D. 2017).

The optimization of aerodynamics in road and rail vehicles has traditionally relied on trial-and-error design methods, where the designer's expertise and experience are used to propose design changes that are expected to lead to improvements (Krajnovic.s.2007).

2.9 Summary of literature review

The summary of literature review is shown in table 2.1.

Table 2.1. Review summary

S/N	Articles	Summary
1	Deaton, L., Rao, M., & Shih, W. Z. (2007).	✓ This paper deals with the effect of wind pressure on the driver and passenger ✓ wind noise is a characteristic pulsating noise generated inside vehicles when they are driven with a side window open. ✓ This low-frequency noise is beyond the human hearing threshold and is perceived by the vehicle occupants as a pulsation or battering causing pressure on the human body, especially the eardrums, and its high sound pressure level becomes so annoying that continued exposure generates intense fatigue.
2	N. Srinivasa Reddy, B. Dhanraj, Sai	✓ Deals with the analysis and calculation of drag force on vehicles with and without wind deflectors.

	Kanishka Annavajjula, et al, (2022).	✓ The model of vehicle chosen here is a truck; it is modeled in the ANSYS work bench designer module. ✓ The vehicle speed is 100 km/hr., and the results obtained show that the total drag coefficient for vehicles without a wind deflector is 0.98 and the total drag coefficient for vehicles without wind deflector is 0.85. Research gap- the analysis is done with only a single vehicle speed (100km/hr.).it will be better if different vehicle speed is considered.
3	Gillespie, P. A., Johnston, J. D., Loriga, M. A., McCaffrey, K. J. W., Walsh, J. J., & Watterson, J. (1999).	✓ this paper deals the relationship between fuel consumption and aerodynamic drag coefficient. ✓ The required power is taken as the product of total resistance force and vehicle speed. ✓ Vehicle with 1.7-liter engine is selected ✓ The result show that a drag coefficient of 0.35, uses 7.1 liters per 100 km while driving at a constant speed of 75 mph. ✓ if the drag coefficient could be decreased to 0.25 and, in turn, reduce the total resistance (rolling and aerodynamic) by 23 percent.
4	Regin A, F., Manimanoharan, M., Reddy, A. B., & Nigam, P. (2013)	✓ Study about Aerodynamic Analysis of Cabriolet Passenger Cars. ✓ In this paper, a modified cabriolet is analyzed and compared with a closed-roof production vehicle. ✓ The flow patterns and the flow velocities both inside and outside the vehicle are studied using a commercial computational fluid dynamics (CFD) solver. ✓ The result shows that the Cabriolet vehicle drag coefficient is about 32% higher than the closed-roof production vehicle.

5	Larisa Dunai, Ismeal Lengua, and Guillermo Peris Fajarnés, (2015)	✓ This paper presents the effect of buffeting noise in passenger cars in real-life conditions at variable speeds. ✓ When a back window is 25% open, the buffeting noise is not perceived; it starts to be perceived when the window is 50% open, with a resonance frequency of 15.6 Hz at a speed of 80 km/h. ✓ When the window is rolled down at 75%, two airflows appear inside the car: one from the top of the upper interior zone and a second one from the central interior zone. ✓ The effect of buffeting noise is then clearly perceived with a resonance frequency of 16.4 Hz at a speed of 80 km/h and a pressure level of 119 dB, increasing to 19.5 Hz at a speed of 110 km/h and a pressure level of 122 db. ✓ At a speed higher than 130–140 km/h, the buffeting noise disappears, depending on the car model.
6	Ivan Gonzalez Casal, (2014).	✓ This paper presents the history of automotive aerodynamics.
7	Abhishek. Patil, Viraj, (2022).	deals with the need for automobile aerodynamics ✓ to reduce fuel consumption. ✓ More favorable comfort characteristics (mud deposition on body, noise, ventilating, and cooling of the passenger compartment). ✓ Improvement of driving characteristics (stability, handling, and traffic safety)

2.10 Research gap

In today's world, vehicles play an important role in the economic growth of a country, and they are considered one of the most important aspects of our daily lives. Due to this, vehicle manufacturers and different researchers seek to improve the performance and comfortability of the vehicles from day to day, and this improvement is done to increase the performance of the engine, transmission line, steering system, driving system, vehicle stability, vehicle aerodynamics, and other vehicle systems. But most improvements are done for luxury vehicle types, and when we come to ordinary vehicles, there are not many improvements in their entire design. Especially if we take the three-wheel Bajaj's, we didn’t see improvements in their body and components. However, three-wheel Bajaj’s are used as the main means of transportation, mostly in undeveloped countries, including Ethiopia. Therefore, this thesis work deals with the design and aerodynamic analysis of a three-wheel Bajaj side wind deflector to create a comfortable means of transportation, to decrease uneven vehicle stability due to one side wind force entering the cabin, to reduce the drag force, and to reduce wind buffeting happening to the three-wheel Bajaj during driving conditions.

CHAPTER THREE

MATERIALS AND METHODS

3.1 Introduction

This chapter includes a description of the materials and methods used in this thesis, outlining the software and computational resources required for the research, the methods followed, and the overall methodology of the study.

3.2 Materials

Table 3.1 shows the material used for this thesis work.

Table 3.1. Materials used

Material name	Use	Specification
software	For 3D modeling	CATIA V5
Software	For the aerodynamic analysis of 3D model	ANSYS
Computer	For documentation and analysis	Processor unit, 8 RAM

3.3 Methodology

The methodology followed in this research aims to analyze and optimize the aerodynamic performance of three-wheeled vehicles, specifically focusing on the role of wind deflectors in reducing drag force and improving vehicle's stability and comfort. The methodology is organized into several stages that collectively help to achieve the thesis objectives. Each stage plays a crucial role in obtaining valuable insights into the vehicle's design and performance under varying conditions. Below is a detailed explanation of each step.

3.3.1. Literature review

The literature study forms the foundation of any engineering research and reviews on the aerodynamic performance of the vehicles. The review includes a detailed analysis of different types of vehicle body designs and their aerodynamic characteristics. Particular attention was given to three-wheeled vehicles, which are known to have unique aerodynamic challenges due to their open structure. These challenges often result in higher drag force, reduced stability, and increased fuel consumption, all of which can be mitigated through design improvements.

The literature study also focuses on understanding the relationship between drag force and fuel consumption. Research suggests that drag force directly impacts fuel efficiency, with higher drag forces leading to higher fuel consumption. Additionally, wind buffeting caused by the vehicle's interaction with air at high speeds is a critical factor that leads to instability and discomfort for passengers. A key area of interest is the use of wind deflectors, which can help reduce drag force and improve aerodynamics by redirecting airflow in a more controlled manner.

The literature review concludes by highlighting various approaches to aerodynamic optimization, such as body modifications and the use of side door wind deflectors, which have been found effective in improving fuel efficiency and reducing drag on vehicles. These findings lay the groundwork for the problem identification stage and inform the design of the 3D model and subsequent analysis.

3.3.**2. Problem identification**

The problem identification stage is the crucial first step in the research methodology, as it involves pinpointing the specific areas of improvement for the three-wheeled vehicle design. Based on the literature study, it was identified that the primary challenge for three-wheeled vehicles is the high drag force, which leads to poor fuel efficiency and instability at higher speeds.

This issue is caused by the vehicle's open structure, which causes uneven airflow around the vehicle and results in wind buffeting. Additionally, the lack of aerodynamic features, such as wind deflectors, contributes to the higher drag forces and the resulting fuel inefficiency. This problem necessitates the need for aerodynamic optimization, particularly through the incorporation of side wind deflectors.

Thus, the problem identified is the inefficiency of the vehicle's aerodynamic design, specifically the excessive drag force and wind buffeting, which affects the overall performance of the three-wheeled vehicle. The goal of the research is to address this issue by implementing a design modification (wind deflectors) and optimizing the vehicle's aerodynamic characteristics.

3.3.3 Modeling

Once the problem has been identified and the literature study has been completed, the next crucial step is to create a 3D model of the three-wheeled vehicle. This model serves as the foundation for the subsequent analysis and optimization stages. The 3D modeling process is conducted using CATIA V5 software, a powerful tool widely used in automotive and aerospace engineering for designing complex geometries and simulating real-world conditions.

The 3D modeling in this study is based on the following key specifications of the vehicle:

- Wheel Base: 2000 mm
- Frame Type: Reinforced Steel Alloy
- Dimensions: Length: 2635 mm, Width: 1300 mm, Height: 1710 mm
- Ground Clearance: 200 mm

These specifications provide the basic framework for the vehicle model, ensuring that the design is both realistic and feasible. The 3D model is created by first constructing the vehicle's frame using reinforced steel alloy as per the specifications. This frame acts as the structural core of the vehicle, and its geometry must be precisely designed to accommodate the components like wheels, suspension, and the powertrain.

The dimensions of the vehicle, including the length of 2635 mm, width of 1300 mm, and height of 1710 mm, are incorporated to create a realistic model of the vehicle’s overall shape. These dimensions are essential for visualizing the vehicle's outer appearance and understanding how the air flows around it. By adhering to these specifications, the model reflects the true size and proportions of the vehicle, which is crucial for the accuracy of the CFD analysis that follows.

The ground clearance of 200 mm plays an important role in the vehicle’s interaction with the air at the lower levels, especially in the wake region, which can influence drag and lift forces. The ground clearance in the 3D model is set to this value to ensure that the undercarriage and airflow beneath the vehicle are realistically represented.

The modeling process also includes the integration of side door wind deflectors. These deflectors are strategically positioned along the vehicle's sides to influence airflow and reduce drag. Their dimensions and positioning are based on aerodynamic principles, ensuring that they redirect air around the vehicle in a way that reduces turbulence and wind buffeting. The design of these deflectors is tested and adjusted to optimize their efficiency.

The 3D model in CATIA V5 also includes detailed parts such as wheels, chassis, and doors, all modeled with precision to ensure they do not interfere with the flow of air around the vehicle. These details are essential for simulating how the vehicle behaves in real-world conditions and ensuring that the resulting aerodynamic properties are accurate.

Once the 3D model is complete, it will serve as the foundation for further analysis in the next stages, where the aerodynamic performance of the vehicle will be tested and optimized. The model will be imported into ANSYS for CFD analysis, where the effects of drag, lift, and airflow will be simulated to evaluate the impact of the wind deflectors and other design modifications.

3.3.4 Analysis

After the 3D model is developed, the next step involves performing aerodynamic analysis using Computational Fluid Dynamics (CFD) software, specifically ANSYS. CFD analysis simulates the interaction of airflow with the vehicle, providing a detailed understanding of how the vehicle moves through the air and how different design features affect aerodynamic performance.

The primary objective of the CFD analysis is to assess the drag force, lift force, and airflow patterns around the vehicle, with and without the wind deflectors. ANSYS provides the tools to visualize the flow of air, identify areas of high turbulence, and analyze the impact of design modifications on aerodynamic performance. During this stage, the drag coefficient (Cd) and lift coefficient (Cl) are computed, which are essential parameters for assessing the vehicle's aerodynamic efficiency.

The analysis will also examine the effect of wind deflectors on wind buffeting, stability, and comfort for the passengers. These insights are crucial for evaluating whether the modifications lead to a significant improvement in fuel efficiency and overall vehicle performance.

3.3.5 Optimization (Response Surface Methodology)

Once the CFD analysis is complete, the next step is optimization. Optimization focuses on adjusting the dimensions and parameters of the 3D model to achieve the best aerodynamic performance. In this research, the optimization is performed using Response Surface Methodology (RSM).

RSM is a statistical technique used to optimize complex processes by approximating the relationship between the design variables (such as the dimensions of the wind deflectors and angle of deflection) and the objective function (such as minimizing drag and lift force). It creates a response surface that maps the relationship between the variables and predicts the outcomes for different parameter combinations.

Through RSM, a set of optimized parameters for the vehicle design is determined, which minimizes drag and lift improves vehicle's stability and comfort. The process involves performing multiple CFD simulations with varying parameters and analyzing the results to find the most effective design configuration. This step is crucial for ensuring that the vehicle's aerodynamic properties are optimized before finalizing the design.

3.3.6 Result and discussion

The discussion stage involves analyzing the results obtained from the CFD analysis and optimization process. The findings are carefully examined to understand the improvements made in the vehicle's aerodynamic performance. The comparison between the vehicle with and without wind deflectors will provide valuable insights into the effectiveness of the modifications.

3.3.7 Comparison

Once the result and discussion are complete, the results from the analysis are compared for two scenarios: one with wind deflectors and one without. This comparison involves evaluating several key aerodynamic parameters:

- Drag Coefficient (Cd): A dimensionless quantity that describes the drag resistance of the vehicle.
- Lift Coefficient (Cl): A dimensionless quantity that describes the lift generated by the vehicle.
- Air Streamline: The visualization of airflow around the vehicle, showing how the wind deflectors influence the air movement.

By comparing these parameters, the effectiveness of the wind deflectors in improving the vehicle's aerodynamic performance can be assessed. This step provides clear evidence of the impact of design modifications on drag reduction and fuel efficiency.

3.3.8 Conclusion and recommendation

The final step of the thesis is the conclusion, which provides a summary of the research findings and the overall outcome of the study. The conclusion emphasizes the improvements made in the vehicle's aerodynamic performance, particularly the reduction in drag force and lift force. The impact of the optimized design on the vehicle's stability and comfort is also highlighted.

Additionally, the conclusion offers recommendations for future research and practical applications of the findings. It suggests further optimization techniques or additional modifications that could improve the vehicle's performance even more. Ultimately, the conclusion summarizes the significance of the research and its contributions to the field of vehicle design and aerodynamic optimization.

3.4 Flowchart

Flowchart of methodology is shown in Figure 3.1.

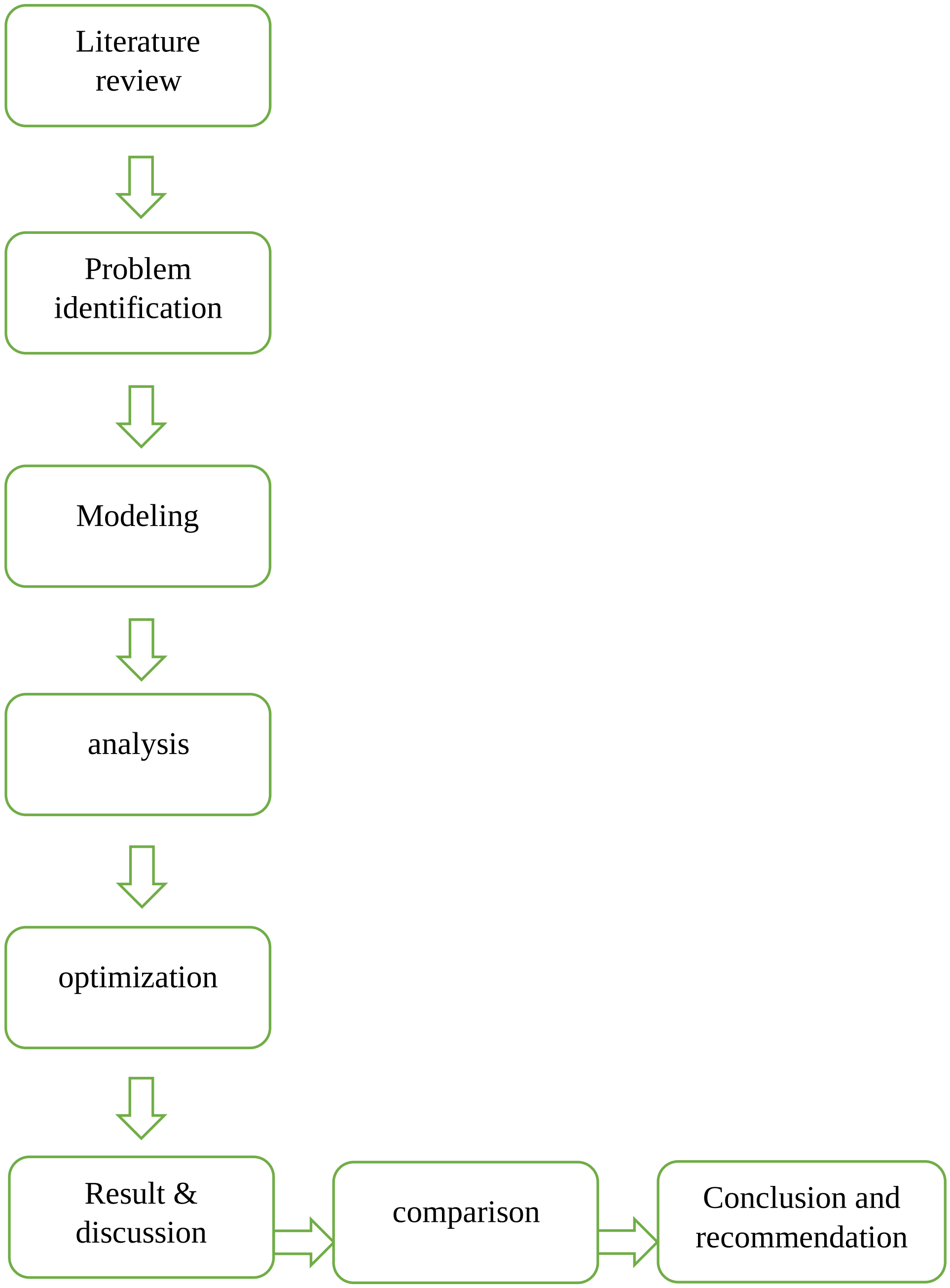

Figure 3.1: Methodology flowchart

CHAPTER FOUR

MODELING AND AERODYNAMIC ANALYSIS OF RE 4S BAJAJ

4.1 CAD Modeling of RE 4S Bajaj

4.1.1 Introduction

To perform the aerodynamic analysis, a 3D CAD model of the RE4S Bajaj is developed using CATIA V5 software. The dimension of the 3D model is taken directly from the existing RE4S Bajaj with the scale of 1:1.

This CAD model is developed based on the outer part of the Bajaj body, and parts like that of the engine, brake line, fuel line, and transmission parts are not included under this CAD model.

The main parts of this CAD model include:

- ✓ Chassis
- ✓ Body
- ✓ Roof

4.1.2 CAD model of chassis

Figure 4.1 Shows the chassis for RE 4S Bajaj. the shape and size of the model is directly taken from the existing Bajaj chassis dimension.

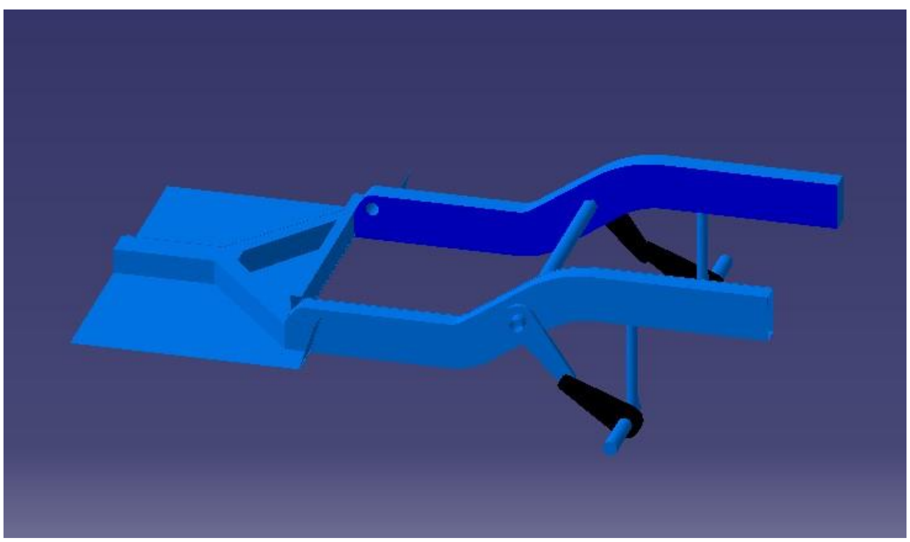

Figure 4.1: Chassis for RE 4S Bajaj

4.1.3 CAD model of body

Figure 4.2 Shows the body for RE 4S Bajaj. the shape and size of the model is directly taken from the existing Bajaj chassis dimension.

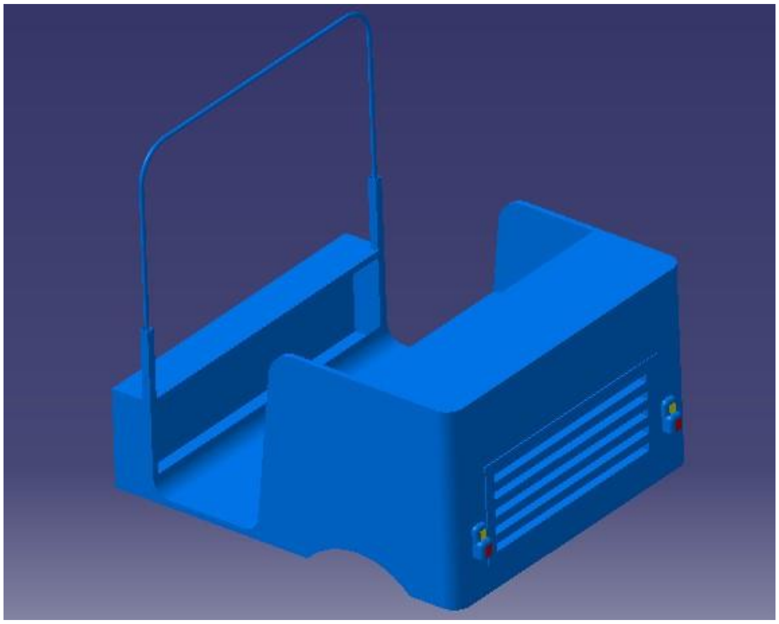

Figure 4.2: Body for RE 4S Bajaj

4.1.4 CAD model of roof

Figure 4.3 Shows the roof for RE 4S Bajaj.

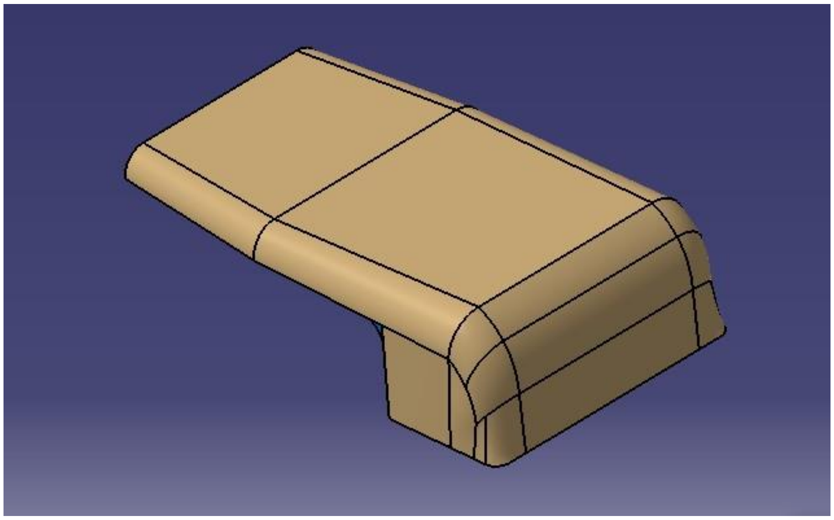

Figure 4.3: Roof for RE 4S Bajaj

4.1.5 CAD model of assembly of RE 4S Bajaj

Figure 4.4 Shows the assembly for RE 4S Bajaj. the 3D model will not include a sub component like that of; side mirror, head lamp this is because the aerodynamic effect of those part is almost negligible.

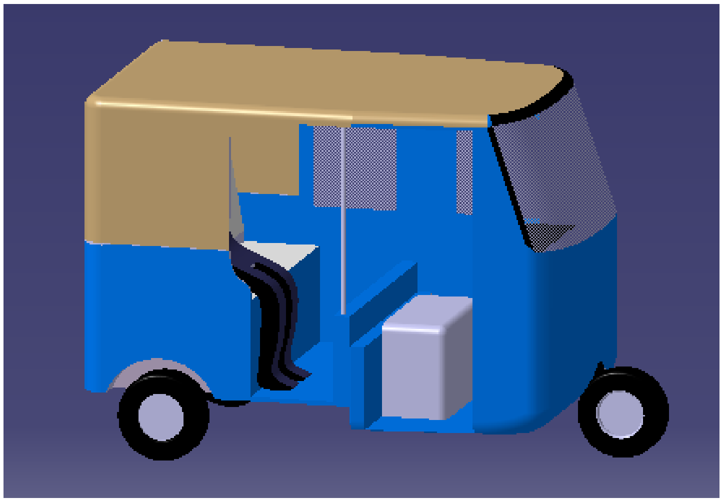

Figure 4.4: Assembly for RE 4S Bajaj

4.1.6 modeling of side wind deflector

The side wind deflector model is used for the aerodynamic analysis of the vehicle. The shape and size of the wind deflector should not have to affect the overall performance of the vehicle. Three different shapes of wind deflector models will be developed, and the one with the minimum drag coefficient is selected.

The type of material used for the wind deflector is acrylic. Acrylic is a transparent plastic known for its exceptional strength, stiffness, and optical clarity. Acrylic sheets are easy to fabricate, bond well with adhesives and solvents, and can be easily thermoformed. Additionally, acrylic offers superior weathering resistance compared to many other transparent plastics.

General Properties of acrylic:

- Relative Density 1.19 g/cm^3
- Rockwell Hardness M 102
- Water Absorption 0.2% /24 hours
- Flammability Class 3

Mechanical Properties:

- Tensile Strength 75 MPa
- Flexural Strength 115 MPa

Thermal Properties:

- Minimum Service Temperature -40ºC
- Maximum Service Temperature 80ºC
- Softening Point > 110ºC
- Linear Expansion 7.7×10-5

Optical Properties:

- ✓ Light Transmission > 92%
- ✓ Refractive Index 1.49

Dimension of wind deflector

The size of the wind deflector depends on the size of the three-wheel Bajaj frontal length. For this thesis work, RE 4S Bajaj is selected. Therefore, the size and shape of the wind deflector have to fit with the size of the RE 4S Bajaj.

The length of the wind deflector is equal to the distance between the lower surface of the three-wheel Bajaj and the upper surface of the three-wheel Bajaj (roof); width of the wind deflector is

Length of the wind deflector = 120 cm.

Width of the wind deflector = (10-20 cm)

NB: The width of the wind deflector is considered to be (10-20 cm) because if it exceeded from 20 cm, it will hide the side mirror.

CAD models of wind deflector

Figure 4.5 shows the CAD models for wind deflector.

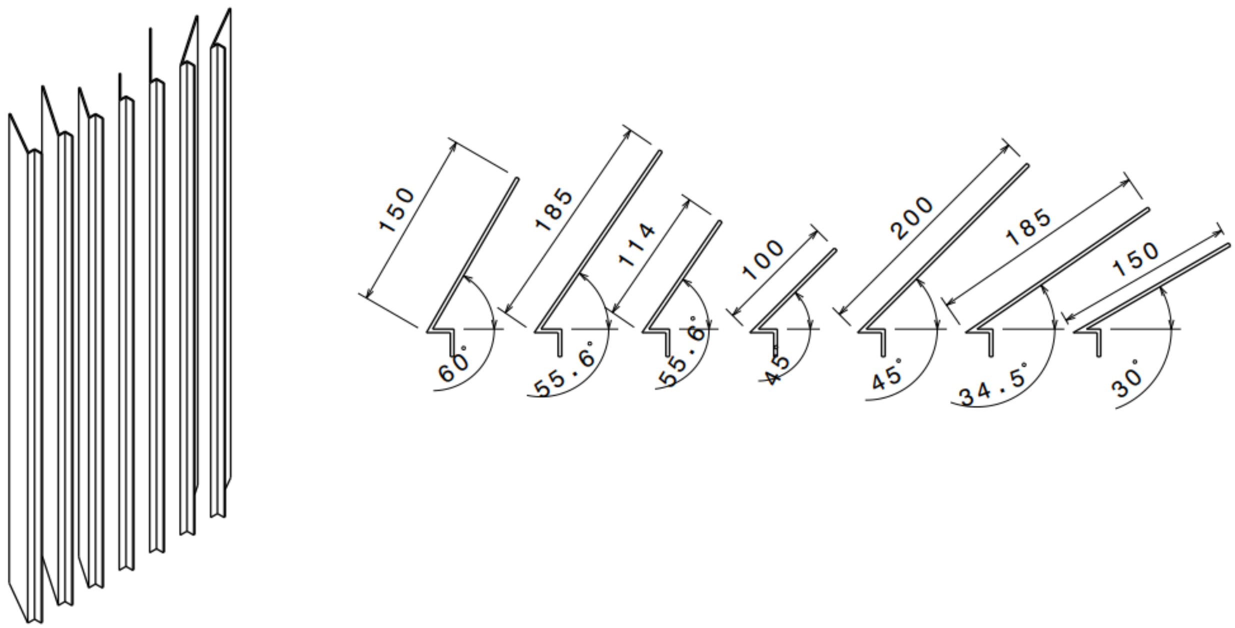

Figure 4.5: seven different CAD models for wind deflector

4.1.7 CAD model of wind deflector assembly with RE 4S Bajaj

Figure 4.6 shows the CAD models for wind deflector assembly with RE 4S Bajaj: -

Figure 4.6: CAD models for wind deflector assembly with RE 4S Bajaj

Figure 4.7 shows the 2D drawing of RE 4S Bajaj with deflector assembly.

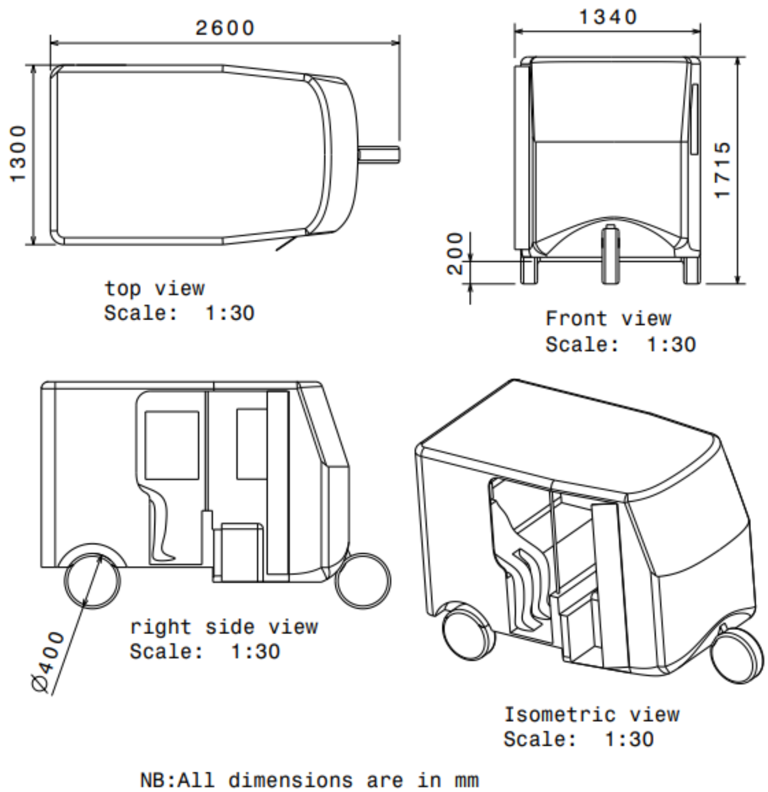

Figure 4.7: Drawing for wind deflector assembly with RE 4S Bajaj

4.2 Design optimization

Design optimization is an engineering design methodology using a mathematical formulation of a design problem to support the selection of the optimal design among many alternatives. For the aerodynamic analysis of the vehicle, we have two input parameters that need to be optimized. The first one is the width of the wind deflector, and secondly, the angle of deflection. The range of wind deflector is between 10 cm and 20 cm, and the range of angle of deflection lies between 30 to and degrees.

The output parameters of the aerodynamic analysis are drag coefficient and lift coefficient. The objective of this design is to design a vehicle with a minimum drag coefficient and minimum lift coefficient; therefore, the value of the input parameters with minimum output parameters is selected using design optimization techniques. In this thesis we use design expert software to conduct the design optimization.

4.2.1 Design expert

Design Expert is a piece of software designed to help with the design and interpretation of multi-factor experiments.

Response surface methodology (RSM): Response surface methodology is a method that is also known as the Box-Wilson methodology. Surface methodology responses are a collection of statistical and mathematical techniques that are useful for modeling and analyzing problems where the response is influenced by various variables (Djimtoingar, S. 2022).

Response surface methodology connects a response or outcome variable (output) to the input data (input) that affect it. If an area with an optimum response is found, a model is made to connect to that area so that the analysis can be carried out to achieve the optimal area.

Input parameters:

- Angle of deflection (minimum value = 30^0 and maximum value = 60^0)
- Deflector width (minimum value = 10 cm and maximum value = 20 cm)

Output parameters:

- Drag coefficient (objective minimum drag coefficient)
- Lift coefficient (objective minimum lift coefficient)

Table 4.1 Combination of input parameters for design optimization

Std	Run	Factor 1 A: deflector angle degree	Factor 2 B: deflector width cm	Response 1 Drag coefficient cd	Response 2 Lift coefficient cl
4	1	55.6	18.53		
8	2	45	20		
5	3	30	15		
2	4	55.6	11.46		
7	5	45	10		
3	6	34.39	18.53		
6	7	60	15		
1	8	34.39	11.4		

The table 4.1 shows eight different combinations of input parameters; therefor, the aerodynamic analysis is carried out for each of the eight combinations, and the optimum input parameters will be selected based on the result of output parameters once the aerodynamic analysis is done.

4.3 Aerodynamic Analysis of CAD Model

4.3.1 Introduction

Aerodynamic analysis is a method that is used to study the aerodynamic characteristics of the vehicles, and the main purpose of the aerodynamic analysis is to design a vehicle with minimum drag and wind noise and prevent undesired lifting force. There are different methods that are used to investigate the performance of vehicle aerodynamics, but the most common include full-size wind tunnels, scale wind tunnels, and computational fluid dynamics (CFD). In this chapter, aerodynamic analysis of the model is performed using CFD analysis because computational fluid dynamics is a relatively cost-effective method that uses computers to test the flow of any liquid or gas, including air. Computational fluid dynamics (CFD) is widely used in a wide range of industries and particularly for the analysis of aerodynamics.

Computational Fluid Dynamics (CFD) technology (ANSYS) is used to study the effect on the vehicle body and flow separation areas. Over the last three decades, Computational Fluid Dynamics (CFD) has gradually joined the wind tunnel and flight test as a primary flow analysis tool for aerodynamic designers (Johnson, F. 2011). To perform the CFD analysis, we use different steps. The ANSYS Fluent software is widely utilized for CFD simulations in various research scenarios, particularly for analyzing the aerodynamics of vehicles (Fikri, A. 2024).

4.3.2 Steps to conduct CFD analysis

The steps that we use to perform aerodynamic analysis of a three-wheel vehicle consist of five main steps; those are:

- Pre-process
- Geometry
- Mesh
- Setup
- Solution
- Result

Pre-Process

Dimension of the vehicle (RE 4S Bajaj)

- Height 1700 mm
- Width 1300 mm
- Length 2634 mm
- Frontal area 2.21 m^2
- Fluid type = air
- Air velocity = 60 km/h
- Enclosure size (X=6m, Y=3m, Z=3m)

The steps followed to conduct CFD analysis in ANSYS are shown in figure 4.8.

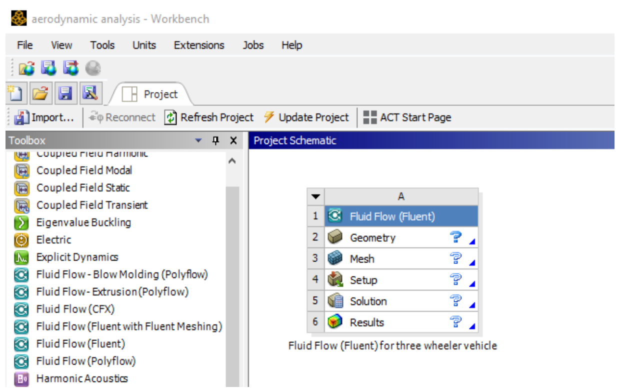

Figure 4.8: Steps in ANSYS aerodynamic analysis

Geometry:

For analysis in CFD, we require a 3D model, which can be modeled using surface modeling software like Creo, CATIA V5, SolidWorks, etc. For this project, CATIA V5 Surface Modeler has been used to develop a 3D model of the car body.

- Converting the CAD file type into an STP file to be convenient for ANSYS software.
- Importing STP CAD file to the geometric section.
- Creating an enclosure using the coordinates of (x=10m, -x=3m, y=5m, -y=0.2m, z=2, -z=2).
- Creating a Boolean operation to subtract the vehicle body from the enclosure.

Meshing:

The process of discretizing a model into a number of elements is known as meshing. It is the most important step in an FEA analysis. The quality of the mesh defines the accuracy of the result. We must require high meshing quality to get crisp and clear elements with uniformity.

- Select the quality of mesh with high meshing quality.
- Create a named selection for (inlet, outlet, enclosure wall, vehicle body).
- Generate mesh using ANSYS Mesh Generator.

The meshing of CAD model with high meshing quality is shown in figure 4.9.

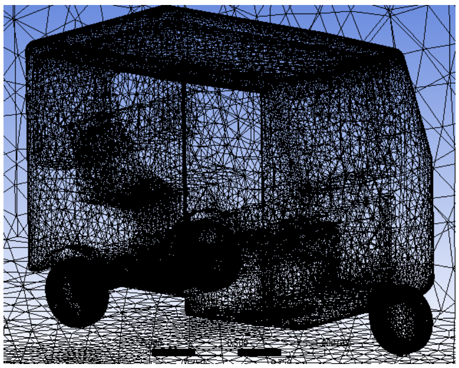

Figure. 4.9: Meshing of CAD model

Setup:

- Select pressure-based solver type.
- Define models (select k-epsilon model).
- Set boundary conditions for all surfaces (inlet = velocity inlet with 60 km/hr, outlet = pressure outlet, enclosure wall = wall solid and vehicle = wall solid).
- Reference value (computed from inlet, vehicle projected area from inlet = 2.04m^2).
- Solution method (pressure-velocity coupling).
- Add report definition (drag coefficient, lift coefficient, drag force, lift force).
- Initialization with 10 iterations.
- Run calculation with 100 iterations.

The Vehicle body, inlet and outlet boundary of the enclosure for the CFD analysis is shown in figure 4.10.

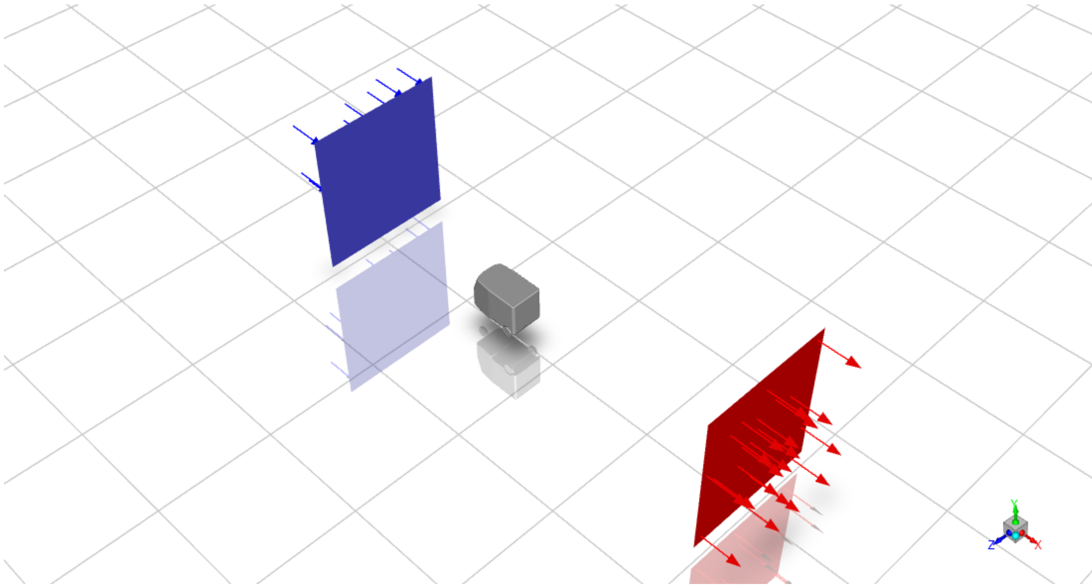

Figure 4.10: Vehicle body, inlet and outlet boundary of the enclosure

Solution:

- Compute the result of the scaled residual, drag coefficient, lift coefficient, drag force and lift force.
- Compute the velocity vector and pressure vector.
- Compute velocity streamline and pressure streamline.

Results:

In the result section we can get graphical representations of different parameters, which are:

- Drag coefficient, lift coefficient, scaled residual.
- Velocity vector and pressure vector
- Velocity streamline

4.3.3 preliminary Aerodynamic analysis of vehicles model.

The first phase of the aerodynamic analysis focuses on an initial assessment of the system's aerodynamic performance. To save computational time, a reduced number of iterations (100) was selected for the preliminary analysis. This approach was particularly useful as there were eight different design scenarios to evaluate. The goal of the preliminary analysis was to quickly identify major aerodynamic characteristics and trends, such as flow patterns, pressure distributions, and drag forces. By performing these initial assessments with fewer iterations, it was possible to narrow down which designs warranted further refinement and optimization. This strategy allowed for an efficient exploration of the design space before committing to more detailed and resource-intensive simulations.

(i)Aerodynamic analysis of vehicles with -out wind deflector.

Figure 4.11 and figure 4.12 show the drag and lift coefficients of the vehicles with a deflector angle of 30^0 and a deflector width of 15 cm.

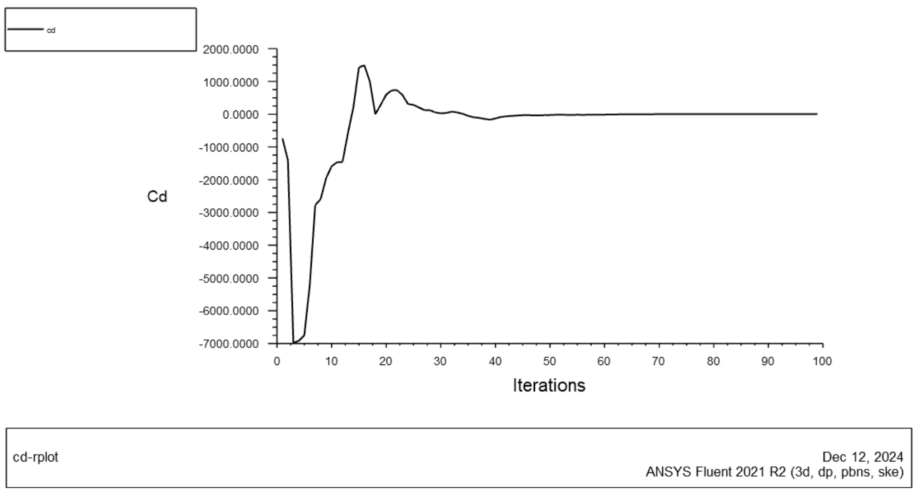

Figure 4.11: Drag coefficient of vehicles without wind deflector (0.65)

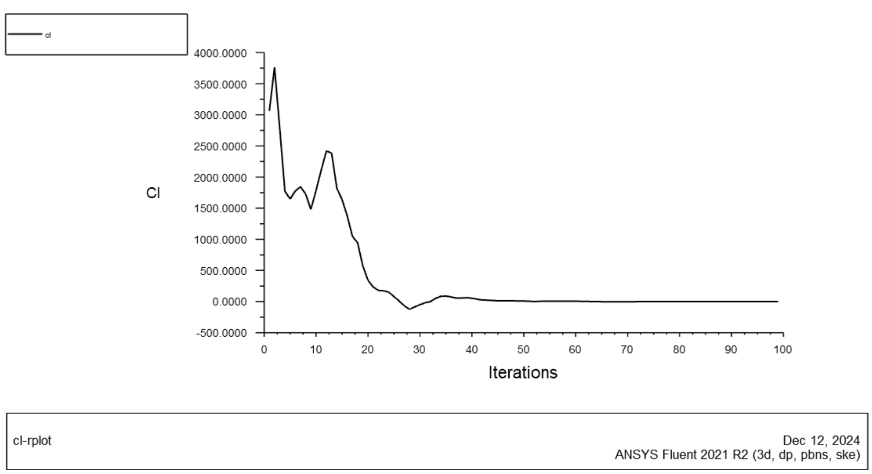

Figure 4.12: Lift coefficient of vehicles without wind deflector (0.26)

(ii) Aerodynamic analysis of vehicles with deflector (width=15cm, θ=30^0)

Figure 4.13 and figure 4.14 show the drag and lift coefficients of the vehicles with a deflector angle of 30^0 and a deflector width of 15 cm.

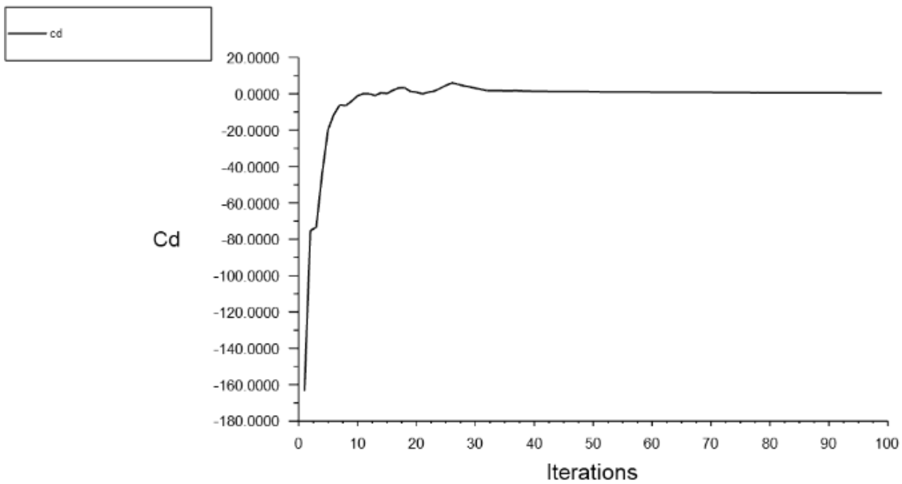

Figure 4.13: Drag coefficient of vehicles (Cd=0.42)

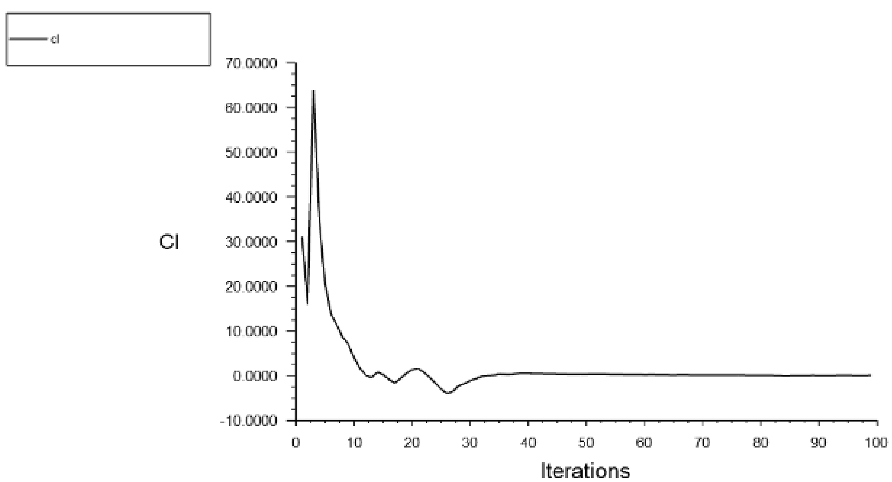

Figure 4.14: Lift coefficient of vehicles (Cl=0.12)

(iii) Aerodynamic analysis of vehicles with deflector (width=18.5cm, θ =34.5^0)

Figure 4.15 and figure 4.16 shows the drag and lift coefficient of the vehicles with deflector angle of 34.5^0 and deflector width of 18.5cm

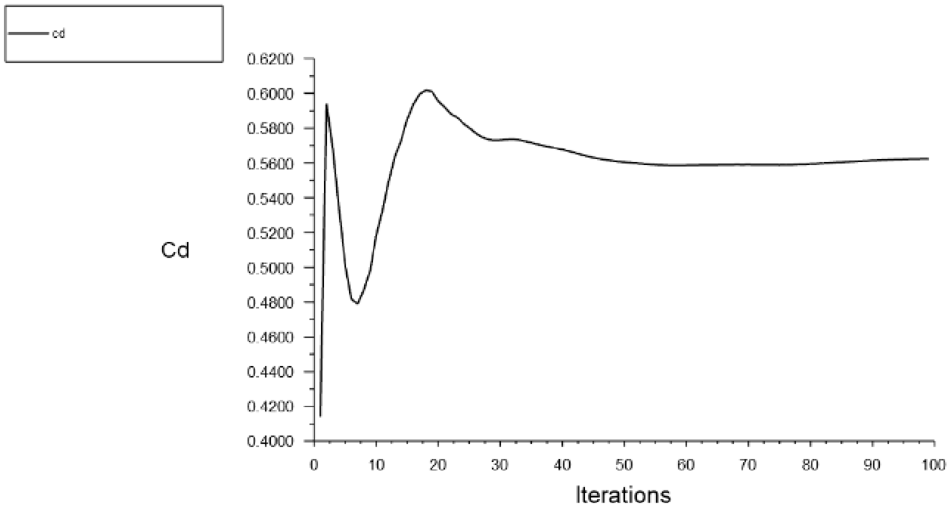

Figure 4.15: Drag coefficient of vehicles (Cd=0.56)

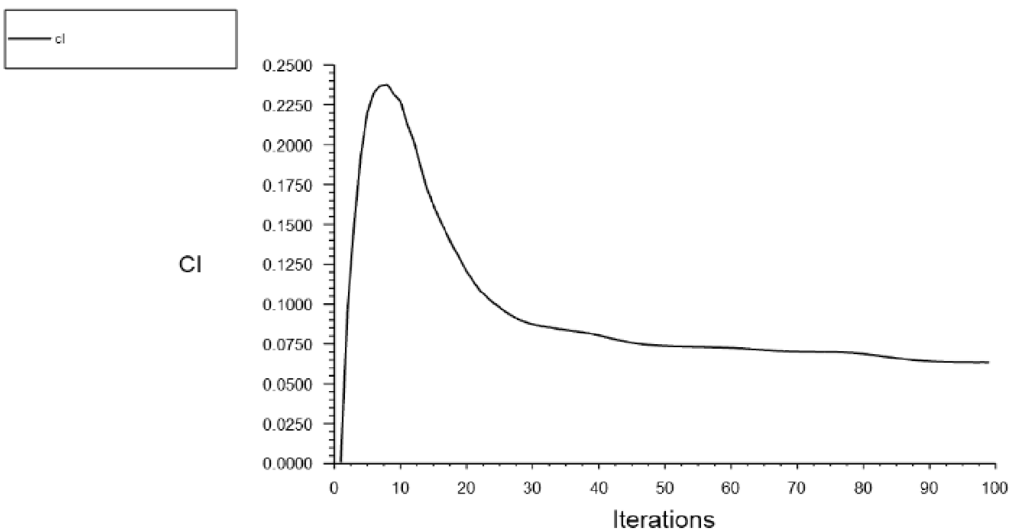

Figure 4.16: Lift coefficient of vehicles (Cl=0.063)

(iv) Aerodynamic analysis of vehicles with deflector (width=20cm $\theta = 45^0$)

Figure 4.17 and figure 4.18 shows the drag and lift coefficients of the vehicles with a deflector angle of 45^0 and a deflector width of 20 cm.

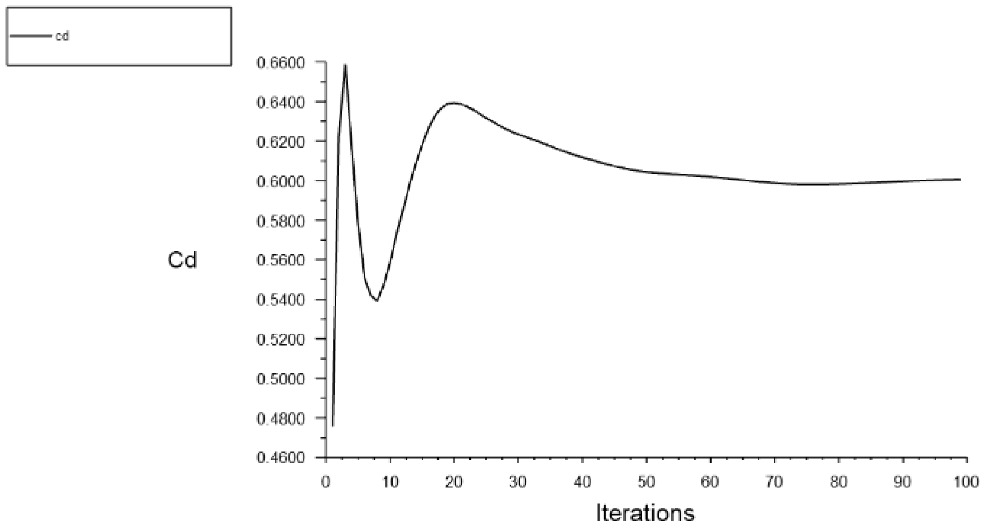

Figure 4.17: Drag coefficient of vehicles (Cd=0.6)

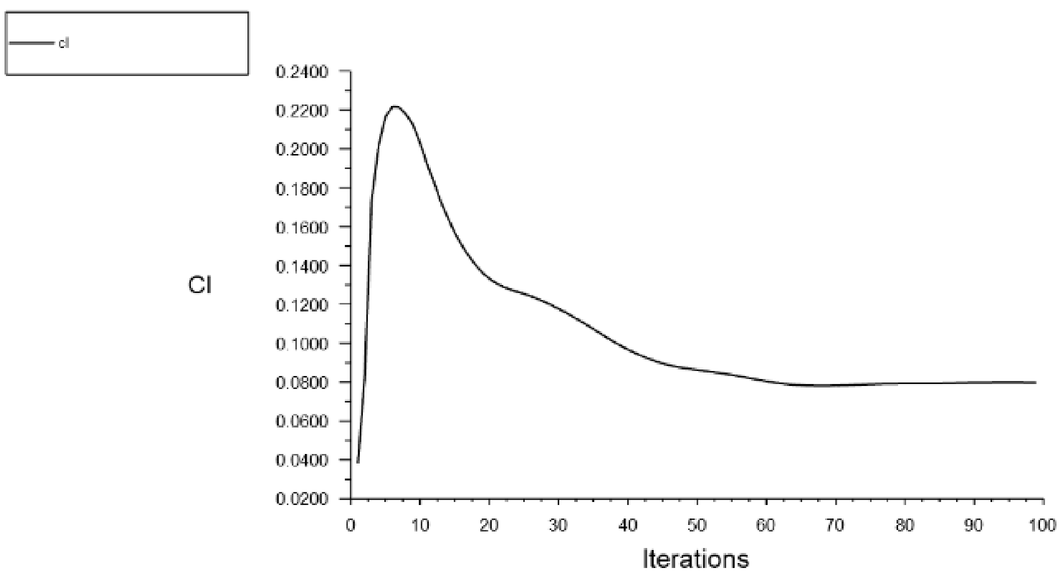

Figure 4.18: Lift coefficient of vehicles (Cl=0.079)

(v) Aerodynamic analysis of vehicles with deflector (width=10cm $\theta = 45^0$)

Figure 4.19 and figure 4.20 show the drag and lift coefficients of the vehicles with a deflector angle of 45^0 and a deflector width of 10 cm.

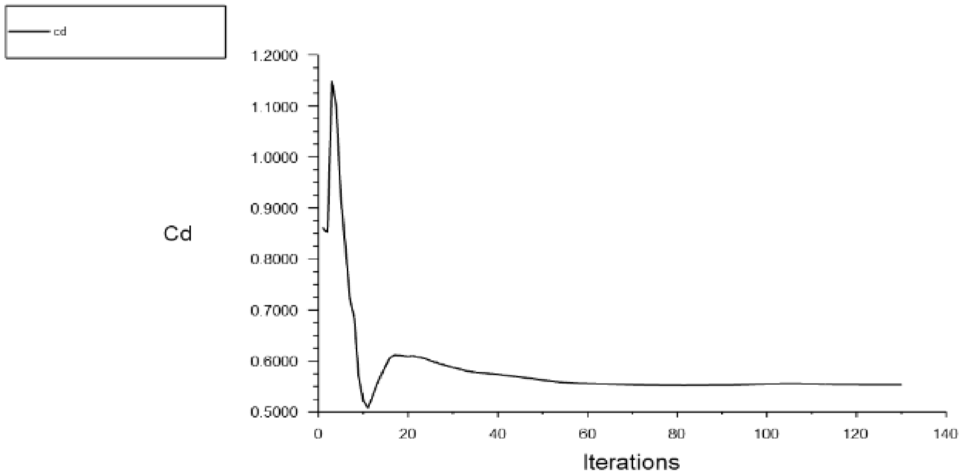

Figure 4.19: Drag coefficient of vehicles (Cd=0.55)

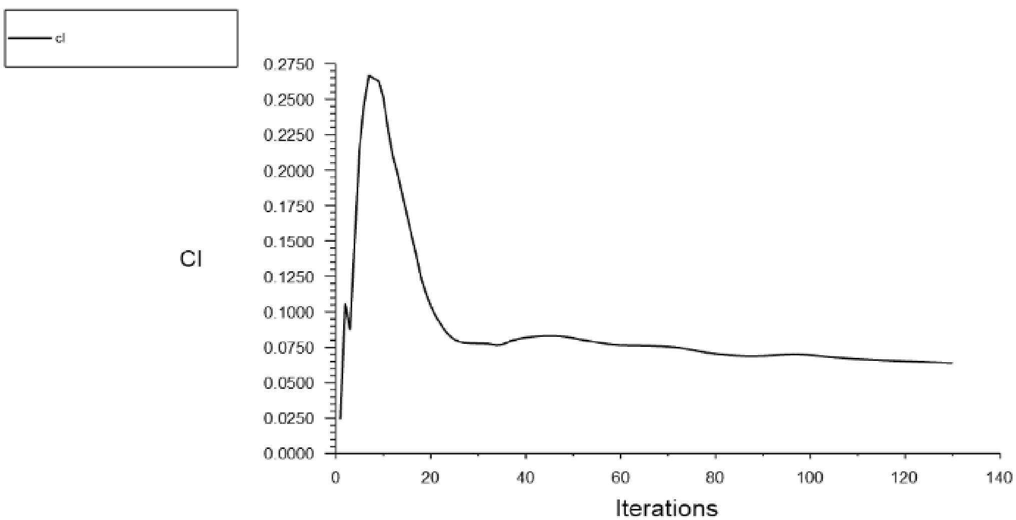

Figure 4.20: Lift coefficient of vehicles (Cl=0.063)

(vi) Aerodynamic analysis of vehicles with deflector (width=11.4cm, $\theta = 55.6^0$)

Figure 4.21 and Figure 4.22 show the drag and lift coefficients of the vehicles with deflector angles of 55.6^0 and deflector width of 11.4 cm.

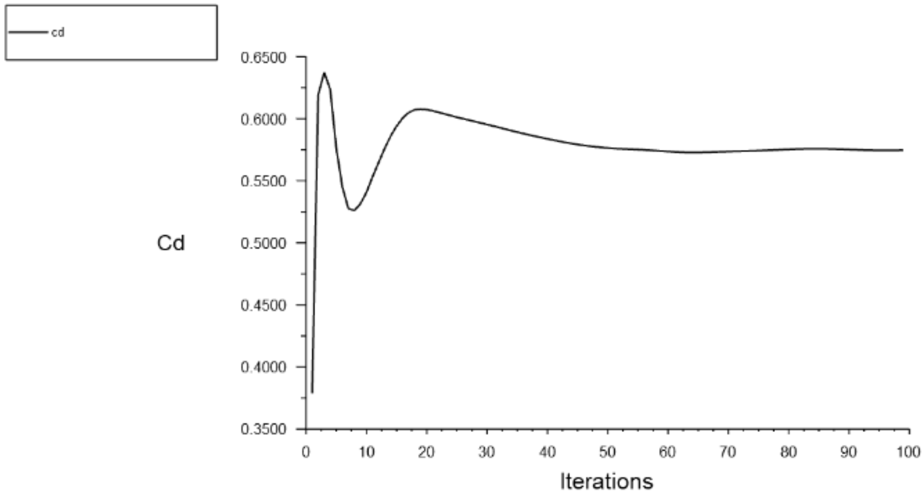

Figure 4.21: Drag coefficient of vehicles (Cd=0.58)

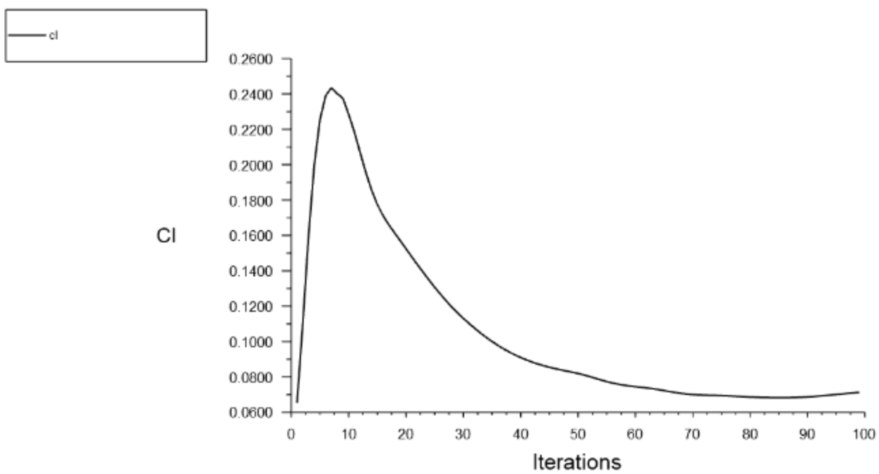

Figure 4.22: Lift coefficient of vehicles (Cl=0.071)

(vii) Aerodynamic analysis of vehicles with deflector (width=18.5cm, $\theta = 55.6^0$)

Figure 4.23 and figure 4.24 shows the drag and lift coefficients of the vehicles with deflector angles of 55.6^0 and deflector width of 18.5 cm.

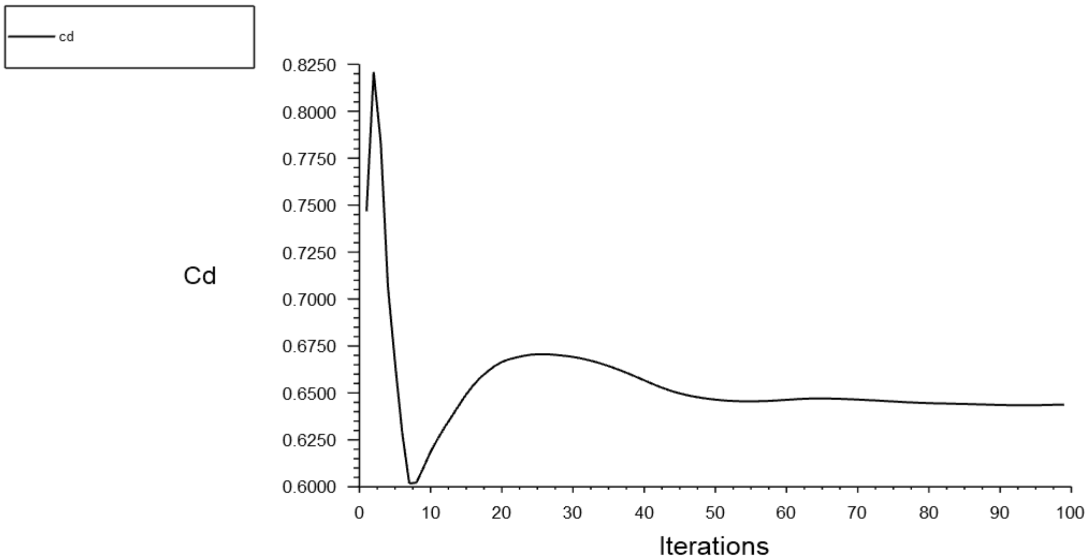

Figure 4.23: Drag coefficient of vehicles (Cd=0.64)

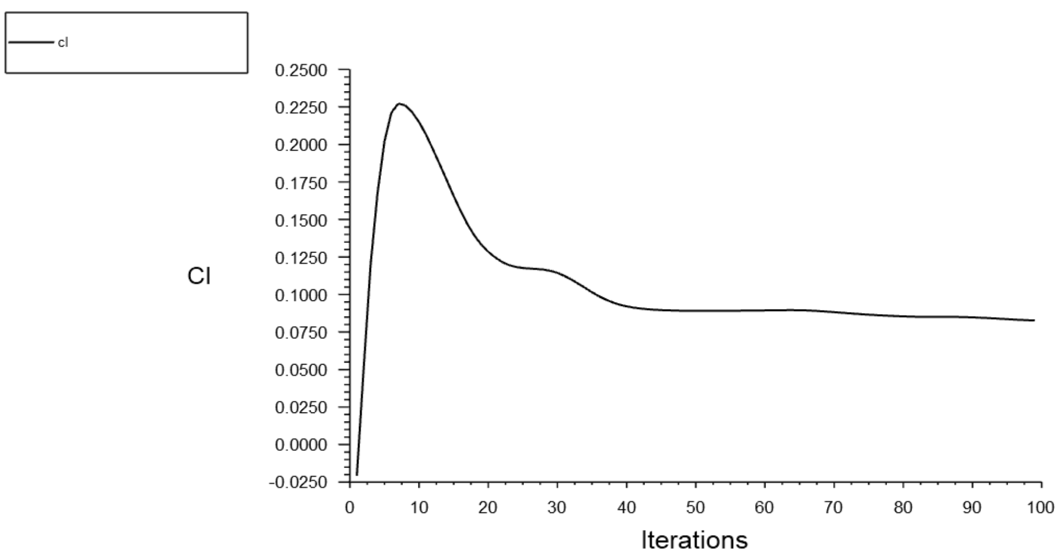

Figure 4.24: Lift coefficient of vehicles (Cl=0.082)

(viii) Aerodynamic analysis of vehicles with deflector (width=15cm, θ =60^0)

Figure 4.25 and figure 4.26 shows the drag and lift coefficients of the vehicles with deflector angles of 60^0 and deflector width of 15 cm.

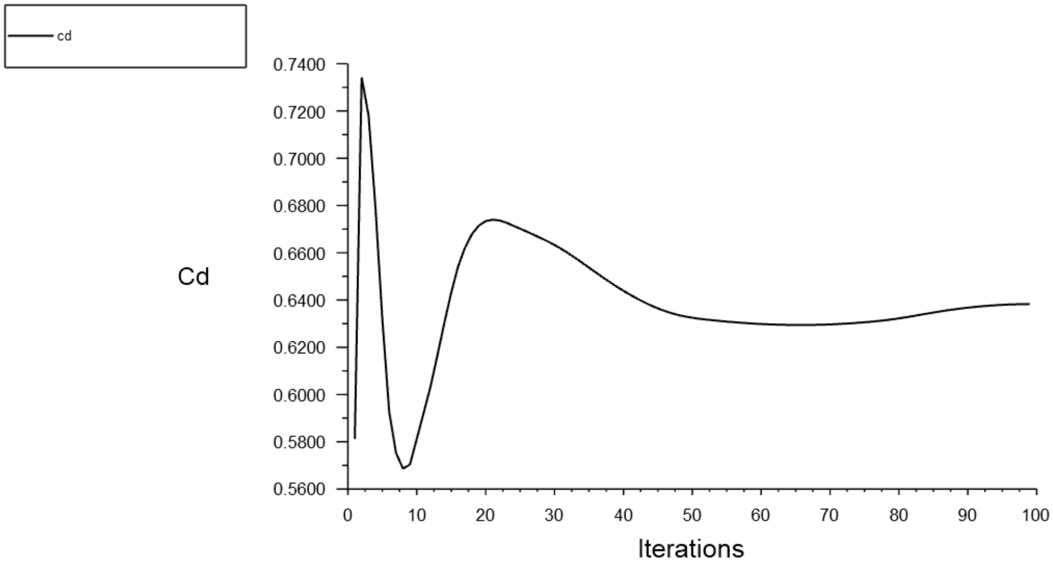

Figure 4.25: Drag coefficient of vehicles (Cd=0.63)

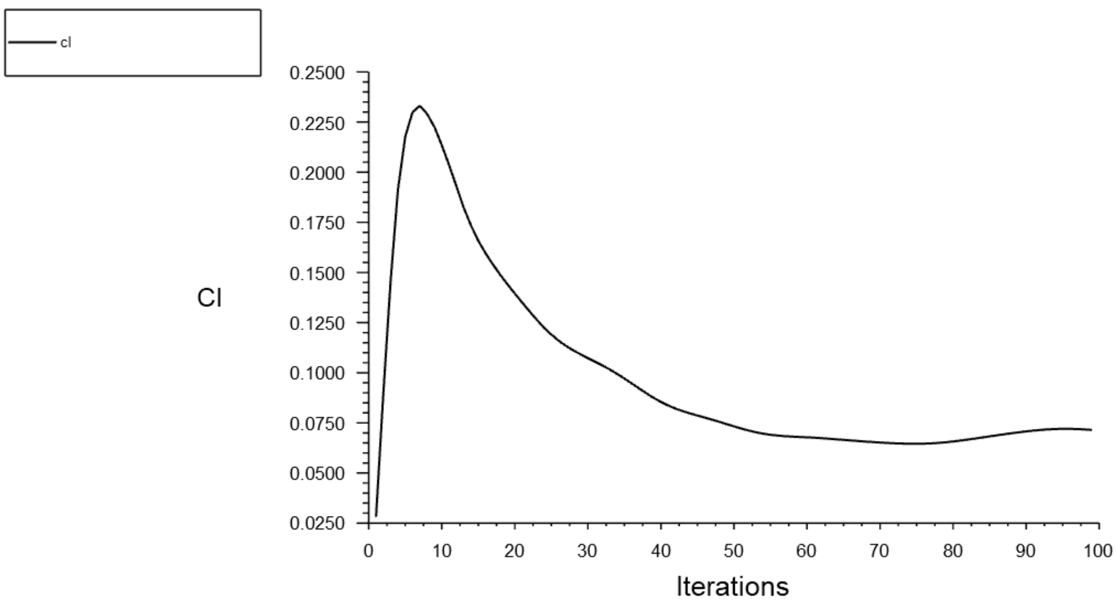

Figure 4.26: Lift coefficient of vehicles (Cl=0.071)

4.4 Response surface design optimization

The table 4.2 shows the summary of input and output parameters that can be used for optimization analysis.

Table 4.2 Summary of CFD analysis results in design expert software

Std	Run	Factor 1 A:deflector angle degree	Factor 2 B:deflector width cm	Response 1 drag coefficent cd	Response 2 lift coefficent Cl
4	1	55.6066	18.5355	0.64	0.082
8	2	45	20	0.6	0.079
5	3	30	15	0.42	0.128
2	4	55.6066	11.4645	0.58	0.071
7	5	45	10	0.55	0.063
3	6	34.3934	18.5355	0.56	0.06
6	7	60	15	0.63	0.071
1	8	0	0	0.65	0.26

4.4.1 Regression equation

Regression equation is a mathematical model that represents the relationship between input (independent) variables and response (dependent) variable. It is used to predict the response variable based on the values of the independent variables. In design of experiment the regression equation helps to model how the factor (independent variables) influences the response (dependent variable).

Types of regression equation and their general equations

Linear regression: it models the relationship between the response and independent variables using the linear term.

$Y=\beta_0 + \beta_1X_1 + \beta_2X_2 + \dots + \beta_k X_k$……………………………………………………. (4)

Quadratic regression equation: includes square term and interaction terms. The quadratic equation for two inputs (independent variables) is given as;

$Y=\beta_0 + \beta_1X_1 + \beta_2X_2 + \beta_3X_1^2 + \beta_4X_2^2 + \beta_5X_1 X_2$…………………………………………. (5)

2FI (Two-factor interaction) regression: It includes linear and interaction terms for two factors. The 2FI equation for two inputs (independent variables) is given as;

$Y=\beta_0 + \beta_1X_1 + \beta_2X_2 + \beta_3X_1X_2$ ……………………………………………………………. (6)

Where Y= response variable (drag coefficient, lift coefficient)

$X_1, X_2, \ldots X_k$ = independent variables (deflector width, deflector angle)

$\beta_0, \beta_1, \beta_2 \ldots \beta_k$= coefficients

from the design expert software, we can see the suggested types of regression equation in the fit summary section.

Table 4.3. Suggested types of regression equation for drag coefficient.

Source	Sequential p-value	Lack of Fit p-value	Adjusted R^2	Predicted R^2	
Linear	0.7263		-0.2319	-6.3020	
2FI	**0.0234**		**0.6324**	**-14.4223**	**Suggested**
Quadratic	0.2832		0.7918		
Cubic					**Aliased**

From table 4.3 the suggested regression equation for drag coefficient is 2FI (Two-factor interaction) regression. therefor the regression equation of the drag coefficient can be written as:

$Y=\beta_0 + \beta_1X_1 + \beta_2X_2 + \beta_3X_1X_2$

Table 4.4 Result of coefficient in terms of actual factor for drag coefficient regression equation

drag coefficent	=
+0.645653	
-0.003776	* deflector angle
-0.020741	* deflector width
+0.000588	* deflector angle * deflector width

Table 4.4 Gives the result of coefficients in the design expert software for drag coefficient regression. once the coefficient values inserted, the regression equation becomes:

$Y_1=0.645653 + -0.00377571 * X_1 + -0.0207414 * X_2 + 0.000588399 * X_1X_2$

Where: Y_1= Drag coefficient regression

X_1= deflector angle

X_2=deflector width

Table 4.5 Suggested types of regression equation for lift coefficient.

Source	Sequential p-value	Lack of Fit p-value	Adjusted R^2	Predicted R^2	
Linear	**0.0099**		**0.7789**	**0.0738**	**Suggested**
2FI	0.0729		0.8877	-0.4138	
Quadratic	0.4927		0.8894		
Cubic					**Aliased**

From table 4.5 the suggested regression equation for lift coefficient is linear regression. therefor the regression equation of the lift coefficient can be written as:

$Y = \beta_0 + \beta_1 X_1 + \beta_2 X_2$

Table 4.6 Result of coefficient in terms of actual factor for lift coefficient regression equation

lift coefficent	=
+0.242126	
-0.002203	* deflector angle
-0.003737	* deflector width

Table 4.6 Gives the result of coefficients in the design expert software for lift coefficient regression. when we inserting the above coefficient values the regression equation become:

$Y_2 = 0.242126 + -0.00220319 * X_1 + -0.00373737 * X_2$

Where: Y_2= Lift coefficient regression

X_1= deflector angle

X_2=deflector width

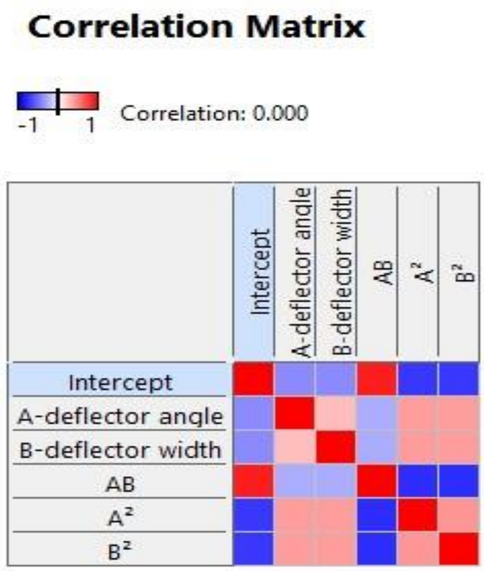

Figure 4.27: Deflector width and deflector angle correlation matrix

From figure 4.27 One can see that the correlation matrix between deflector angle and deflector width is below zero (-Ve); this shows the correlation between these two parameters is weak.

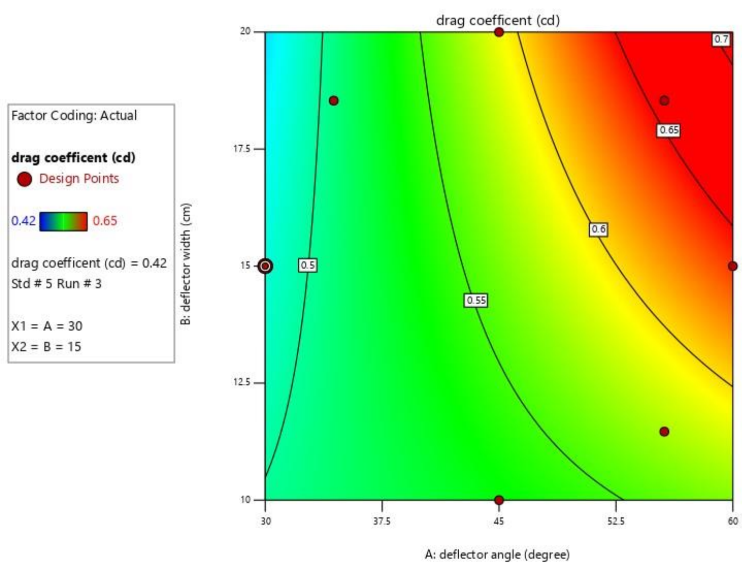

Figure 4.28: Drag coefficient contour plot

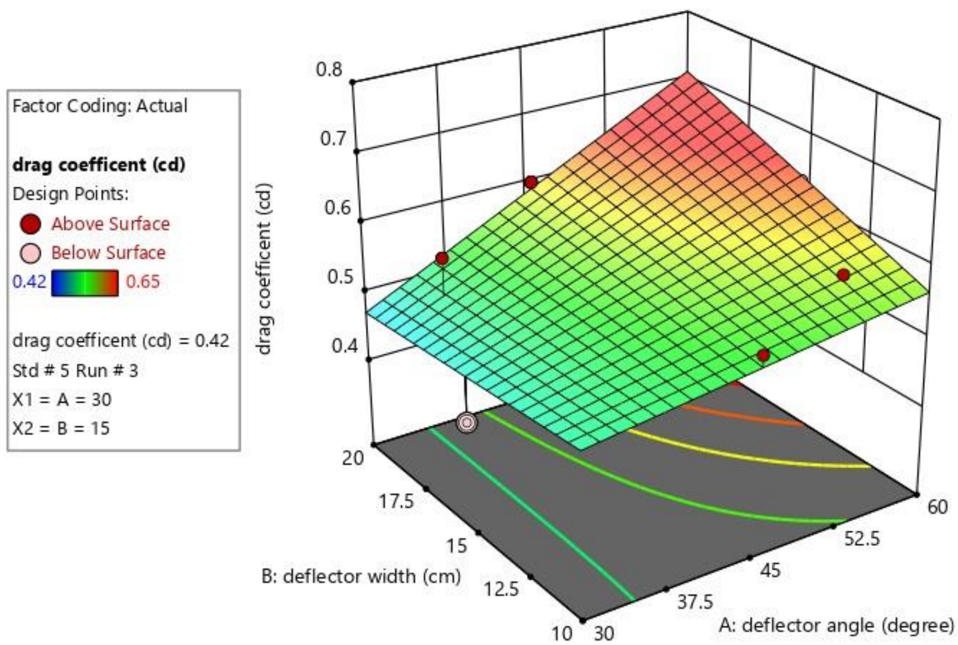

Figure 4.29: Drag coefficient 3D plot

Figures 4.28 and figure 4.29 show the drag coefficient contour and 3D plot, respectively. The result obtained shows a minimum drag coefficient of 0.42 in the blue color area, and this value of drag coefficient is achieved with a deflector width of 15 cm and a deflection angle of 30^0.

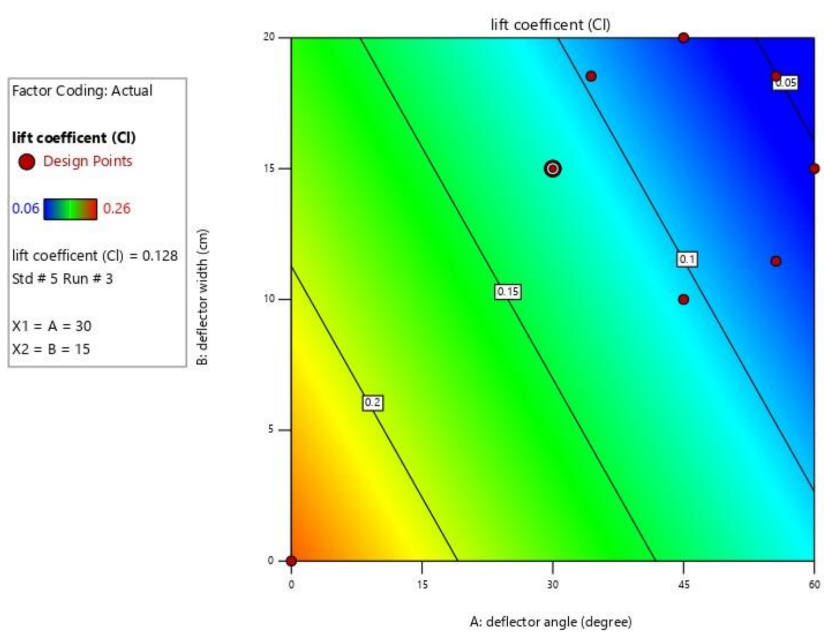

Figure 4.30: Lift coefficient contour plot

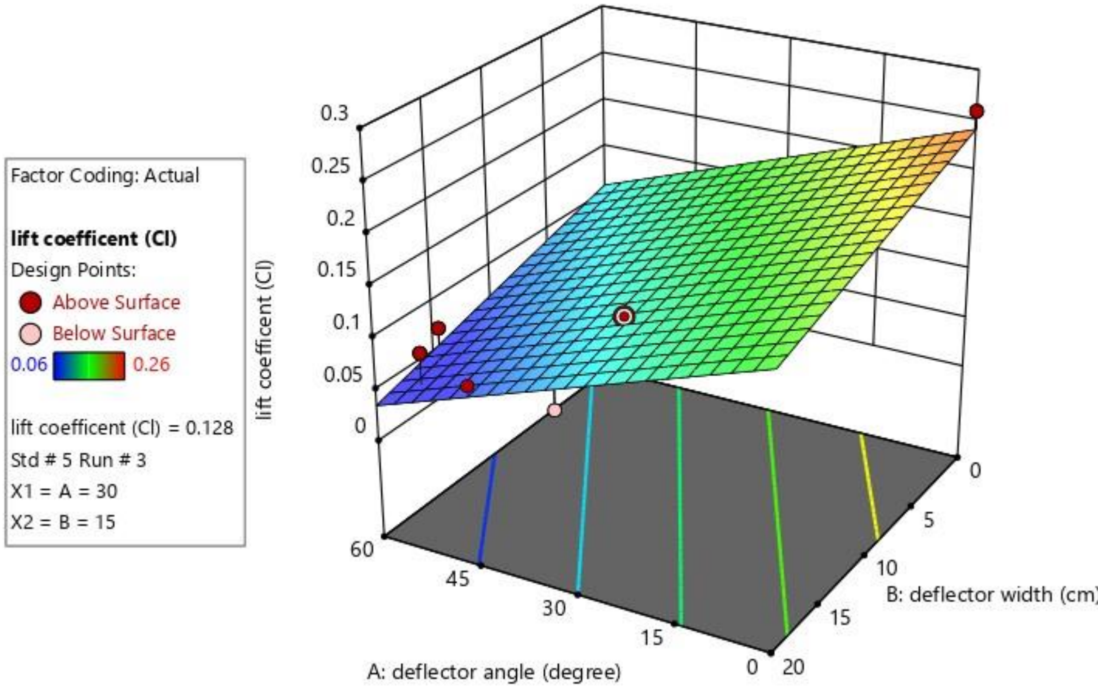

Figure 4.31: Lift coefficient 3D plot

Figures 4.30 and figure 4.31 above show the lift coefficient contour and 3D plot, respectively. The result obtained shows a minimum lift coefficient of 0.12 in the blue color area, and this value of drag coefficient is achieved with a deflector width of 15 cm and a deflection angle of 30^0.

4.4.2 Selection of the vehicle model with best aerodynamic performance (minimum drag and lift force)

From the Figure 4.28 drag coefficient contour and Figure 4.30 lift coefficient contour plot above, we have seen that there is a huge difference with the results of drag and lift coefficient obtained from the aerodynamic analysis. The aerodynamic performance of a vehicle is mainly affected by the drag and lift forces exerted on the vehicle body. In order to have good aerodynamic performance, it's essential to reduce the effect of the drag and lift force. Therefore, in this thesis, a vehicle model with a deflector angle of 30^0 and a deflector width of 15 cm is selected because this vehicle model has a minimum drag force of 149.2 N and a minimum lift force of 44.6 N.

4.5 Detailed Aerodynamic Analysis for optimized result

Following the preliminary analysis, the results were optimized, and a more detailed, refined analysis was conducted with 400 iterations. In this phase, only two design scenarios were evaluated: the optimized vehicle design and the vehicle without the wind deflector. This focused analysis with a higher number of iterations enabled a more accurate and thorough evaluation of these specific configurations. The increased iterations ensured a precise understanding of the aerodynamic behavior of the optimized design and the baseline model, providing a comprehensive comparison of their performance in terms of drag, stability, and overall aerodynamic efficiency. By dedicating more computational resources to these two scenarios, a deeper insight into the effects of the optimization and wind deflector could be gained.

4.5.1 Aerodynamic analysis of vehicles with-out wind deflectors

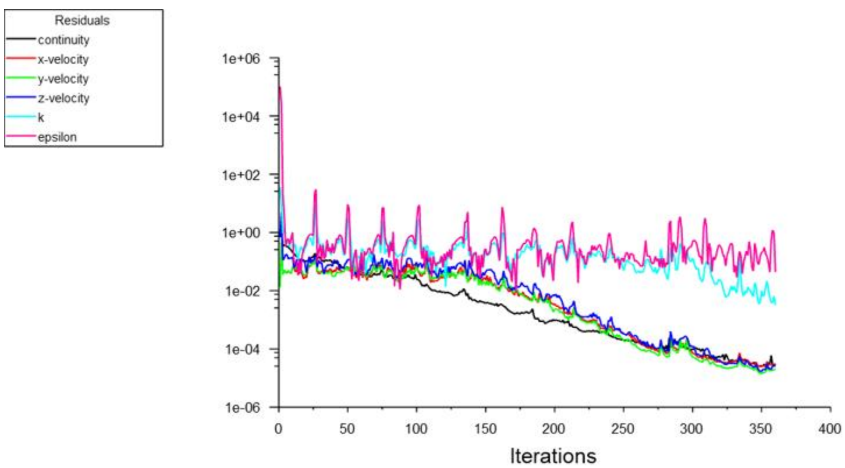

Figure 4.32: Scaled residual

The figure 4.32 Shows the scaled residuals of x, y, and z velocity and the continuity of the aerodynamic analysis. The values of the x, y, and z velocities and continuity are below zero, which indicates the convergence of the analysis. If the value of the scaled residual is above zero, then it indicates the divergence of the analysis.

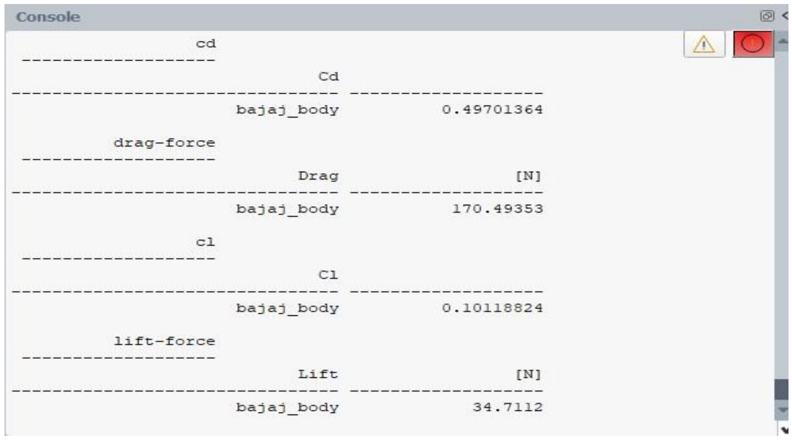

Figure 4.33: Print console for Cd and Cl

The Figure 4.33 shows the print console of the analysis, which shows the exact values of the drag force and lift force of the analysis. This table is used when the estimation of drag and lift force becomes difficult from the drag and lift graph.

Figure 4.34 show the drag and lift coefficients of the vehicle without a wind deflector.

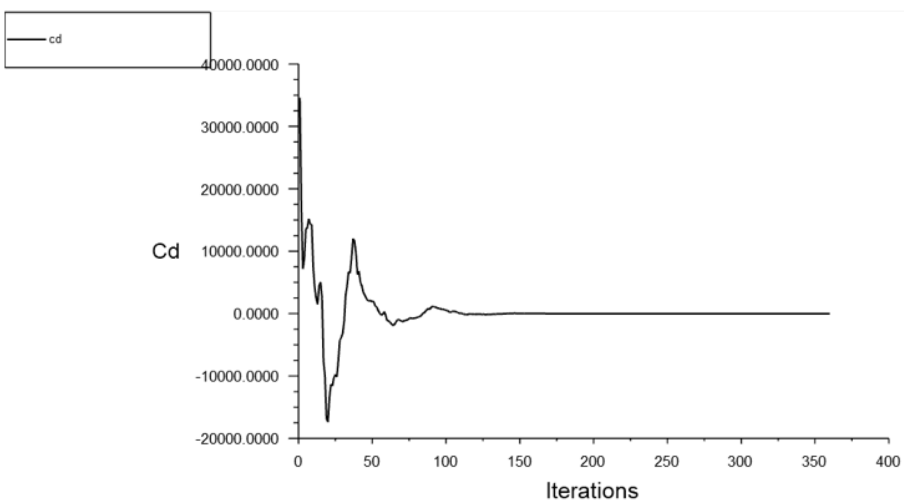

Figure 4.34: Drag coefficient of vehicles (Cd=0.49)

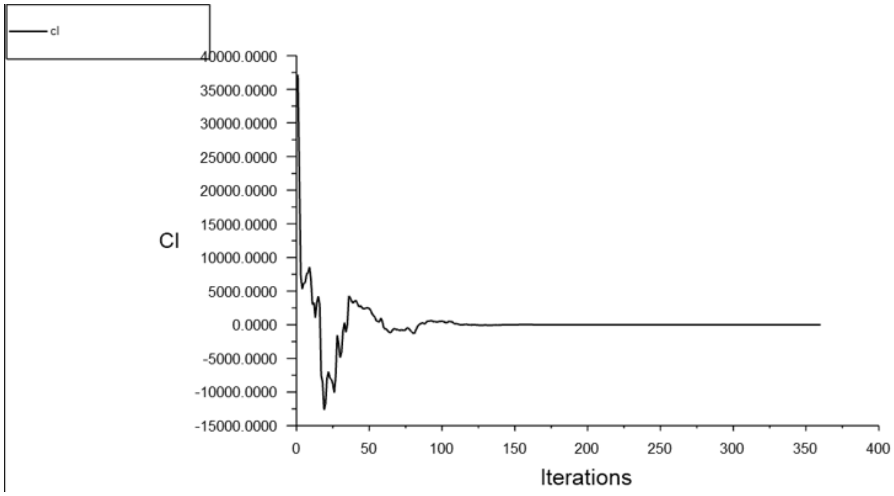

Figure 4.35: Lift coefficient of vehicles without wind deflector (0.1)

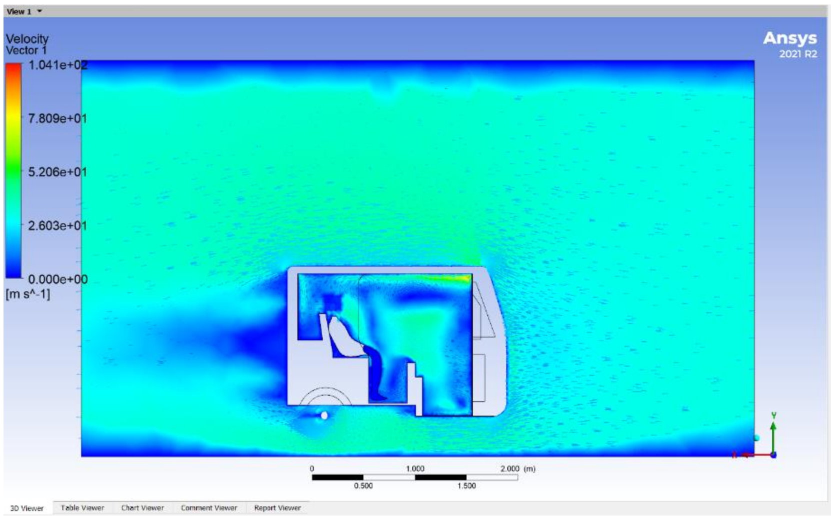

Figure 4.36: Velocity vector distribution around the vehicle body (for vehicle without wind deflector)

Figure 4.36 shows the velocity vector distribution around the model. The red region represents the high-velocity region, the blue region represents the low-velocity region, and the dark blue region represents zero velocity. The results show that minimum air velocity 0 m/s is distributed in the inside vehicle, top and bottom of the enclosure wall, and rear areas of the vehicle. The airflow speed increases, with the front and top part of the car at this point having the highest value of speed reached at the back of the passenger seat, the velocity is very low.

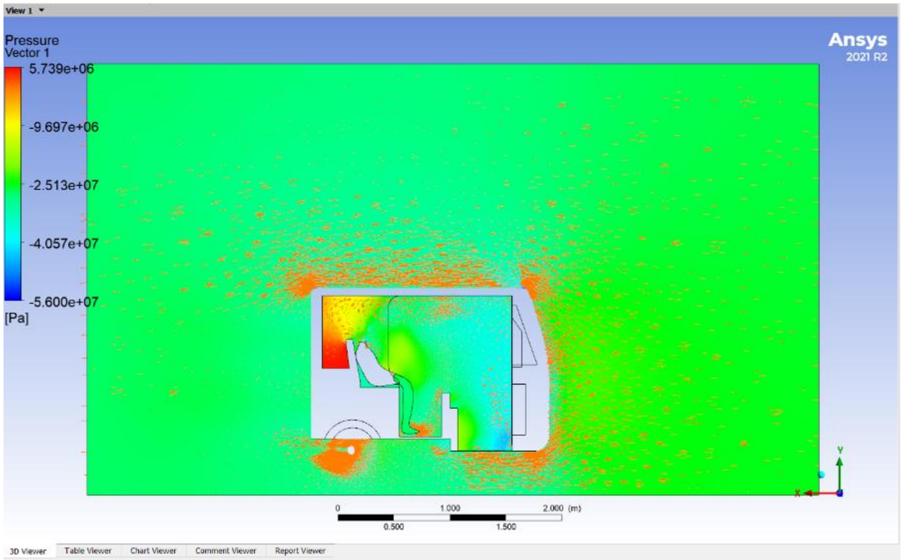

Figure 4.37: Pressure distribution of the car model

Figure 4.37 shows the pressure vector distribution in the aerodynamic duct simulation area inside the contours. The light blue area represents low pressure, and the red area is high pressure. The area at the back of the passenger seat has a highest-pressure concentration of 5.7 bar because the air entering inside the vehicle is stored here, and there is no passing way; due to this, it starts to move in a backward direction, which creates maximum pressure. The rear side of the vehicle and area of the driver seat has minimum values of pressure because a vacuum will be created at that point.

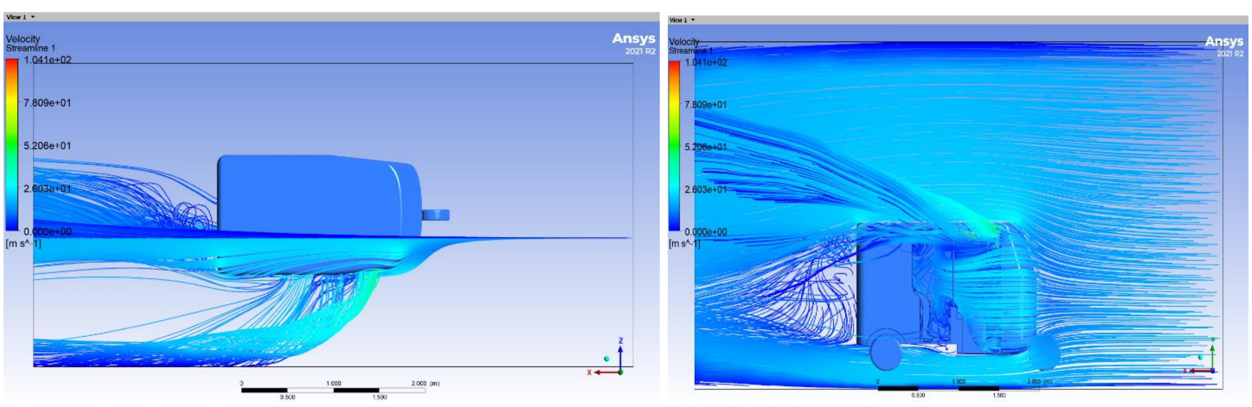

Figure 4.38: Velocity Stream line of cad model

From the figure 4.38 one can visualize that the streamline of airflow is not laminar; the air flows from the inlet side and is deflected by the frontal area of the vehicle, and then it enters inside the vehicle, which results in the disturbance of airflow.

4.5.2 Aerodynamic analysis of vehicles with deflector (width=15cm, θ=30^0)

Figure 4.39 shows the scaled residual of the vehicles with deflector angle of 30^0 and deflector width of 15cm.

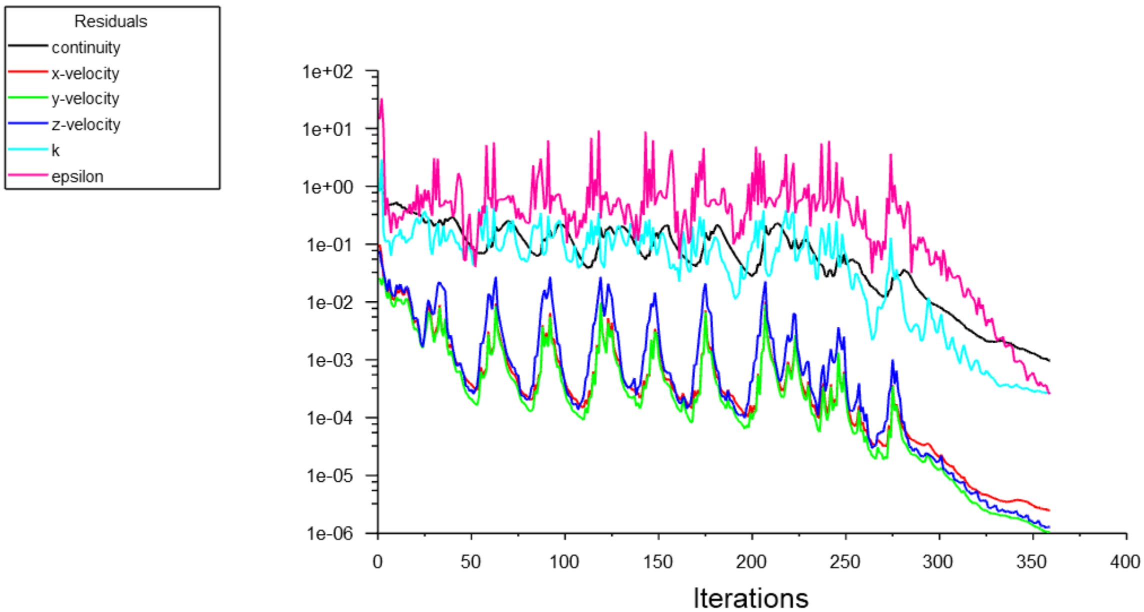

Figure 4.39: Scaled residual

From above figure 4.39 the scaled residuals of x, y, and z velocity and the continuity of the aerodynamic analysis is shown in different color. The values of the x, y, and z velocities and continuity are below 1e-04, which indicates the convergence of the analysis.

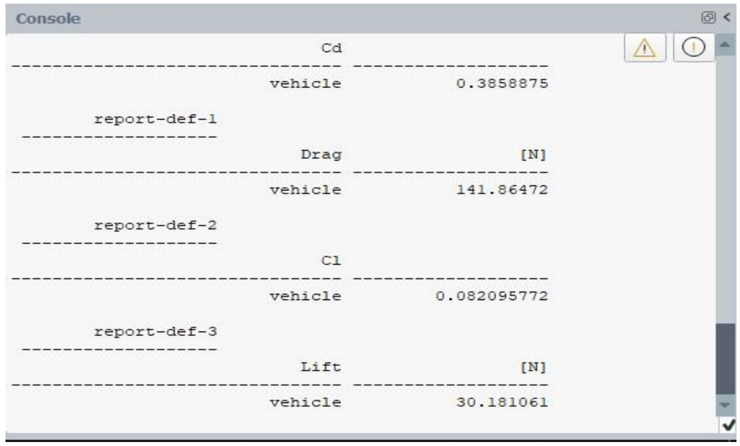

Figure 4.40: Print console for Cd and Cl

The Figure 4.40 shows the print console of the analysis, which shows the exact values of the drag force and lift force of the analysis. This table is used when the estimation of drag and lift force becomes difficult from the drag and lift graph.

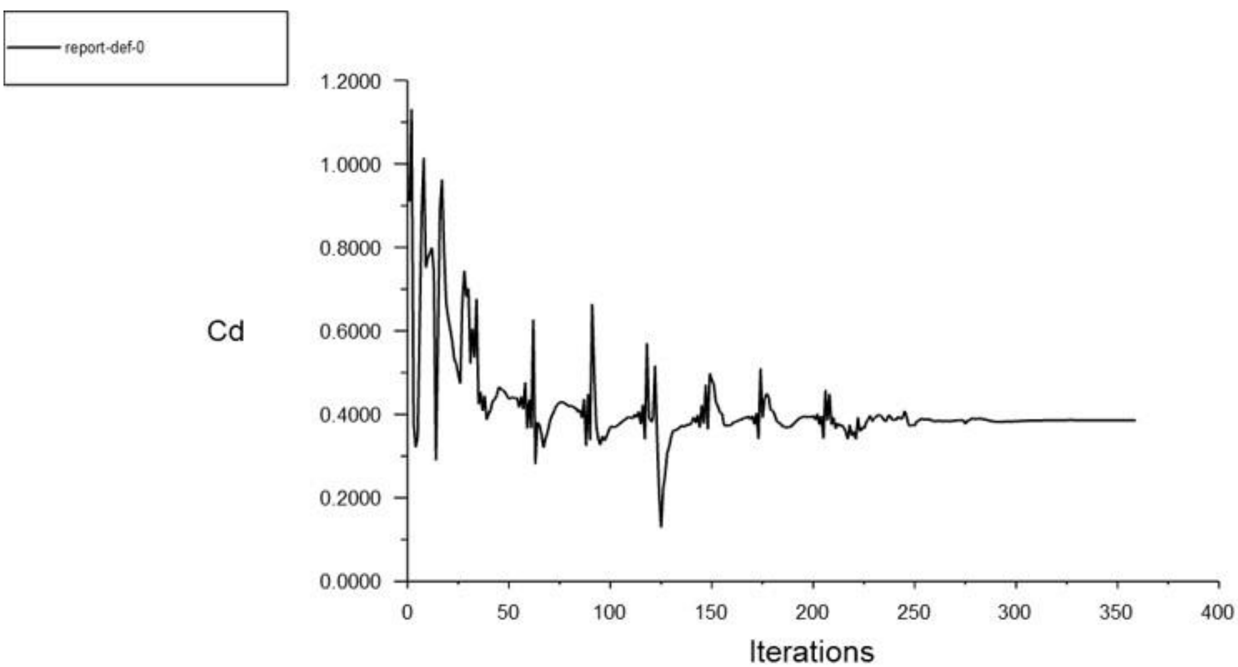

Figure 4.41: Drag coefficient of vehicles (Cd=0.38)

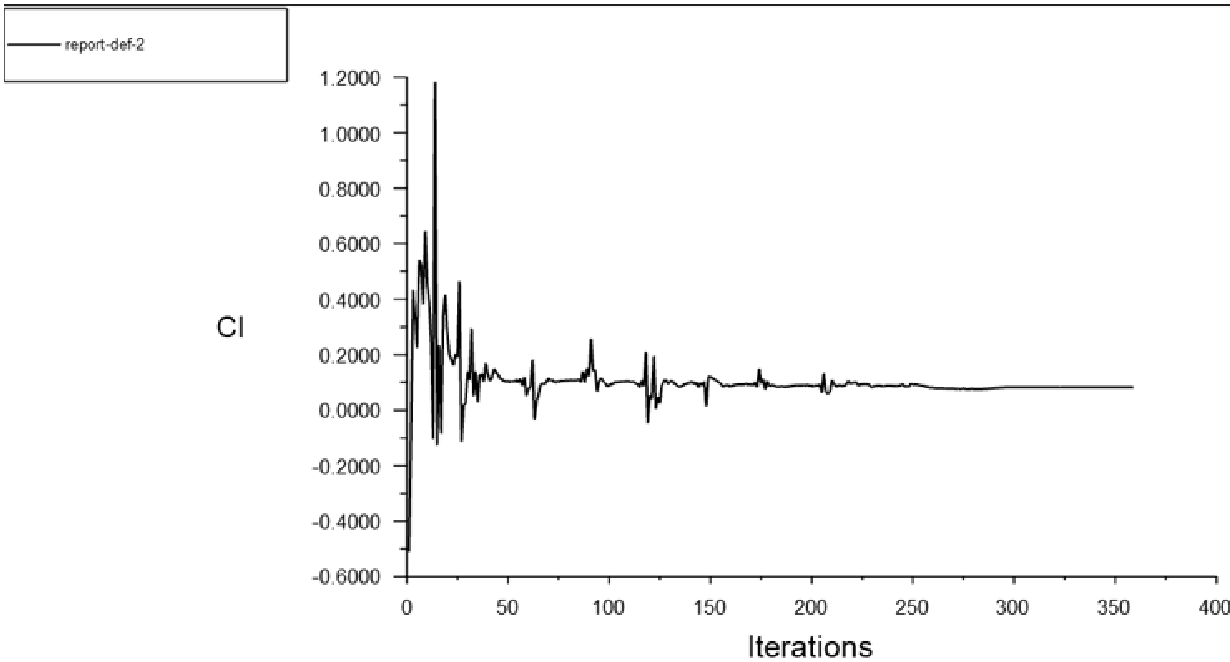

Figure 4.42: Lift coefficient of vehicles (Cl=0.08)

Figure 4.41 and figure 4.42 show the drag and lift coefficients of the vehicles with a deflector angle of 30^0 and a deflector width of 15 cm.

Figure 4.43: Velocity distribution around the vehicle body

Figure 4.43 shows the velocity vector distribution around the model for vehicles with 15 cm deflector width and a 30^0 angle of deflection. It shows the velocity vector with a maximum velocity of 70 m/s at the front edge of the vehicle and a minimum velocity of 0 m/s at the back of the passenger seat and at the rear side of the vehicle body. We can also see the velocity inside the vehicle lies between 17 m/s and 0 m/s. which indicates the reduction of velocity of air when compared to the air velocity of the vehicle without a wind deflector.

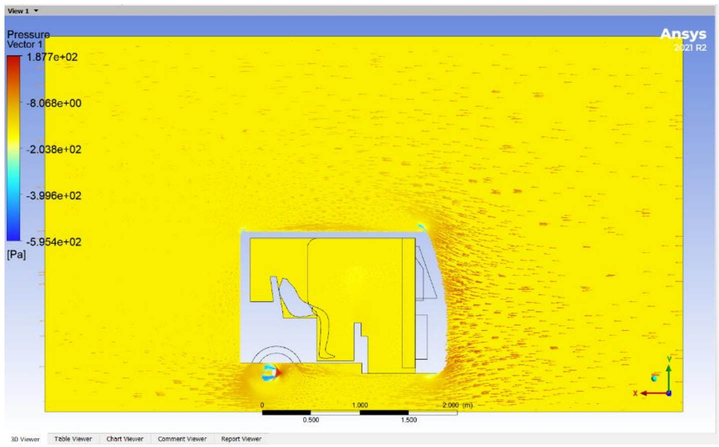

Figure 4.44: Pressure distribution of the car model

Figure 4.44 shows the pressure distribution through the vehicle body. From fig we can see the highest pressure (187 Pa) occurring at the front, top, and bottom of the vehicle surface. Inside the vehicle and the rear side of the vehicle show minimum values of the pressure vector. There is a reduction of pressures when compared to the air pressure of vehicles without wind deflectors. The area around the rear wheel shows the minimum values of (-594 Pa).

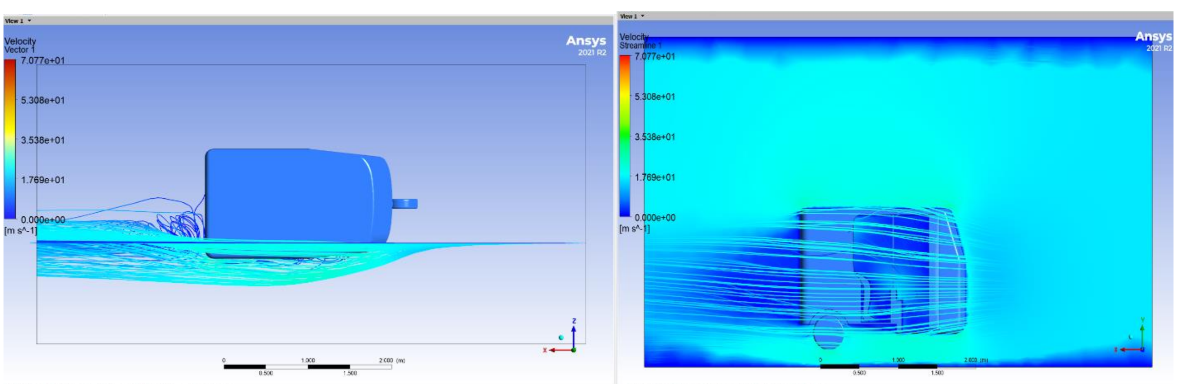

Figure 4.45: Velocity Stream line of CAD model

The figure 4.45 shows the streamline of air velocity; as we can see, the streamline of the air is laminar when we compare it to the vehicles without a wind deflector. The laminar flow of the air stream line results in the reduction in wind noise (wind buffeting).

CHAPTER FIVE

RESULT AND DISCUSSION

5.1 Result of Drag and Lift Force

Table 5.1 Gives the comparison of drag force, drag coefficient, lift force, and lift coefficient of the vehicle with and without a wind deflector at an initialization phase of 10 iterations, followed by a run phase of 100 iterations for different eight combination of deflector width and deflector angle.

Table 5.1 Summary preliminary analysis

S.No	Type of vehicle	Drag coefficient	Drag force in N	lift coefficient	Lift force in N
1	Vehicle without a wind deflector (0 cm and 0^0)	0.65	262.71	0.26	105
2	vehicles with a deflector angle of 30^0 and a deflector width of 15 cm	0.42	149.2	0.128	44.6
3	vehicles with a deflector angle of 34.5^0 and a deflector width of 18.5 cm	0.56	200	0.06	22.69
4	vehicles with a deflector angle of 45^0 and a deflector width of 20 cm	0.6	219.5	0.079	29.16
5	vehicles with a deflector angle of 45^0 and a deflector width of 10 cm	0.55	191	0.063	22.01
6	vehicles with a deflector angle of 55.6^0 and a deflector width of 11.4 cm	0.58	204.12	0.071	25.42
7	vehicles with a deflector angle of 55.6^0 and a deflector width of 18.5 cm	0.64	237.3	0.082	30.42
8	vehicles with a deflector angle of 60^0 and a deflector width of 15 cm	0.63	229.5	0.071	25.6

Table 5.1 shows maximum (drag coefficient = 0.65, lift coefficient = 0.26, drag force = 262.71 N, and lift force = 105 N) for the vehicle without a wind deflector and minimum (drag coefficient = 0.42, drag force = 149.2 N) for vehicles with a deflector angle of 30^0 and a deflector width of 15 cm. Vehicles with a deflector angle of 45^0 and a deflector width of 10 cm have a minimum lift coefficient of 0.063 and a minimum lift force of 22.01 N. For the vehicle with a wind deflector, the values of drag force and lift force increase when the angle of deflection increases from 30^0 to 60^0; this is due to the increasing of the frontal projection area of the vehicle.

Table 5.2Gives the comparison of drag force, drag coefficient, lift force, and lift coefficient for Detailed Aerodynamic Analysis of the vehicle without a wind deflector and a vehicle with a deflector angle of 30^0 and a deflector width of 15 cm at an initialization phase of 100 iterations, followed by a run phase of 400 iterations.

Table 5.2 Summary of drag force, drag coefficient, lift force and lift coefficient for detailed analysis

S.N	Type of vehicle	Drag coefficient	Drag force in N	lift coefficient	Lift force in N
1	Vehicle without a wind deflector	0.49	170.49	0.1	34.71
2	vehicles with a deflector angle of 30^0 and a deflector width of 15 cm	0.38	141.86	0.08	30.18

The results show a significant improvement in aerodynamic efficiency with the wind deflector, as evidenced by the reduction in both drag coefficient and drag force. The drag coefficient decreases from 0.49 for the vehicle without the deflector to 0.38 with the deflector, indicating a smoother airflow around the vehicle. This lower drag coefficient translates directly into a reduction in drag force, which drops from 170.49 N to 141.86 N. The reduction in drag force by approximately **28.63 N** corresponds to a **16.8%** reduction, suggesting that the wind deflector effectively reduces air resistance, potentially improving fuel efficiency and overall vehicle performance by requiring less energy to overcome aerodynamic drag.

In terms of lift, the vehicle with the wind deflector also demonstrates improved stability, as reflected by the reduction in both lift coefficient and lift force. The lift coefficient decreases from 0.1 to 0.08, which indicates that the vehicle experiences less upward aerodynamic force, a favorable outcome for stability. Similarly, the lift force decreases from 34.71 N to 30.18 N, a **13.14%** decrease, showing that the deflector helps maintain a more grounded vehicle posture. By reducing lift, the deflector enhances handling and control, ensuring that the vehicle remains more stable and less prone to aerodynamic-induced lift, especially at higher speeds.

5.2 Comparison of the selected vehicle model with vehicle without wind deflector

5.2.1 Comparison of fluid flow stream line diagram

Figure 5.1 and figure 5.2 below show the streamlines of the fluid flow around the vehicle for the vehicle with and without a wind deflector.

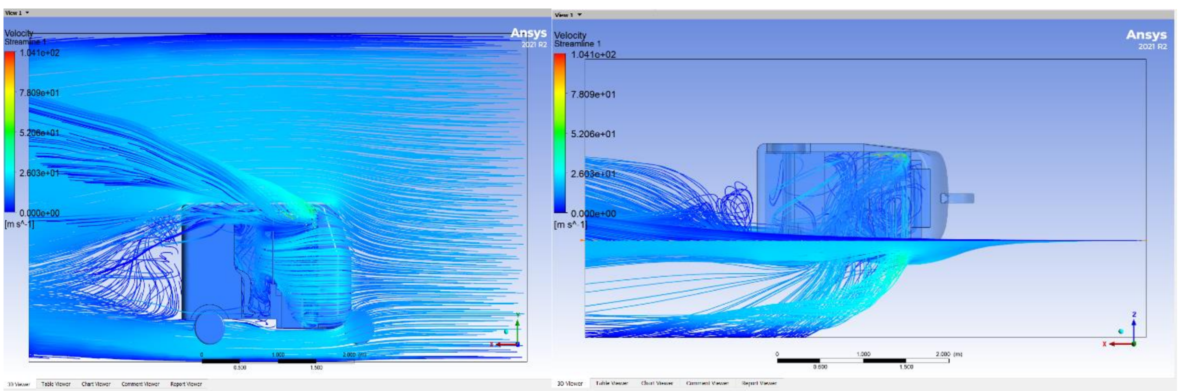

Figure 5.1: Fluid flow stream line for the vehicle without wind deflector

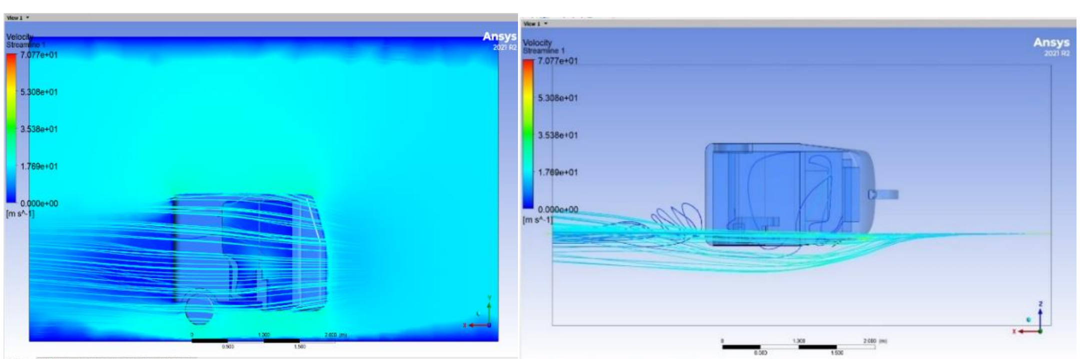

Figure 5.2: Fluid flow stream line for the vehicle with deflector angle of 30^0 and deflector width of 15cm

In Figure 5.1 the airflow is disturbed as it hits the frontal area of the vehicle. This deflection causes the airflow to enter the vehicle's interior, disrupting the smooth, laminar flow. As a result, the airflow inside the vehicle becomes turbulent, which increases wind pressure inside the compartment. Passengers inside the vehicle experience higher wind resistance due to this turbulent airflow.

Figure 5.2 in this case, the vehicle is equipped with a wind deflector. The deflector redirects the incoming air, preventing most of the airflow from entering the interior of the vehicle. This redirection reduces the disturbance inside, resulting in smoother airflow and a noticeable reduction in wind pressure within the vehicle. Consequently, the passengers would experience less wind pressure, improving comfort inside the vehicle.

In summary, the presence of a wind deflector in Figure 5.2 helps to guide the airflow around the vehicle, reducing the internal wind pressure that passengers would face compared to the scenario in Figure 5.1, where the lack of such a deflector leads to higher internal pressure due to disturbed airflow.

5.2.2 Comparison of velocity vector

Figure 5.3 and figure 5.4 below show velocity vector for vehicle with and without wind deflector.

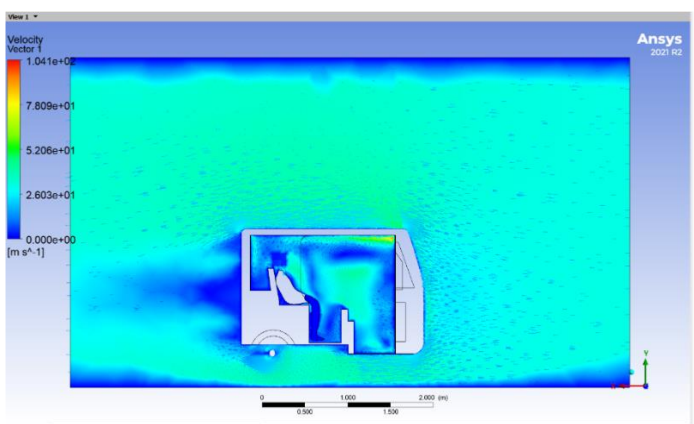

Figure 5.3: Velocity vector for vehicle without wind deflector.

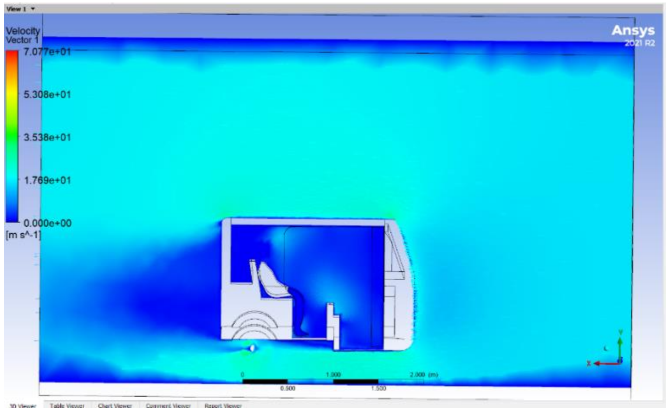

Figure 5.4: Velocity vector for vehicle with wind deflector of (width=15cm, θ=30)

Figure 5.3 in this scenario, the airflow inside the vehicle shows a distribution of low air velocity along the top and bottom walls of the vehicle enclosure, as well as in the rear areas. The air velocity gradually increases as it moves towards the front and top parts of the car, where it reaches its highest value. This pattern suggests that the air is entering from the front of the vehicle and accelerating as it moves toward these regions. However, at the back of the passenger seat, the airflow velocity drops significantly or becomes zero. This happens because the air entering the vehicle is obstructed, causing it to stop and reverse direction due to a lack of space or passage for the fluid flow.

Figure 5.4 shows a more uniform distribution of air velocity within the vehicle, ranging from 17 m/s to 0 m/s. The reduction of air entering the vehicle contributes to this uniformity, as less airflow is introduced into the interior. The uniform distribution likely results from design features such as the introduction of a wind deflector or other aerodynamic modifications that control the airflow, ensuring that it does not disturb the interior as much as in the previous case. The range of air velocities suggests a more controlled and consistent airflow inside the vehicle.

In summary, Figure 5.3 presents a scenario where the airflow is highly variable, with areas of high velocity at the front and top, and stagnation or reverse flow at the rear due to obstruction. On the other hand, Figure 5.4 depicts a more uniform and controlled airflow distribution, with a smooth velocity range, resulting from efforts to reduce the amount of air entering the vehicle.

5.2.3 Comparison of pressure vector

Figure 5.5 and figure 5.6 below show the pressure vector for a vehicle with and without a wind deflector.

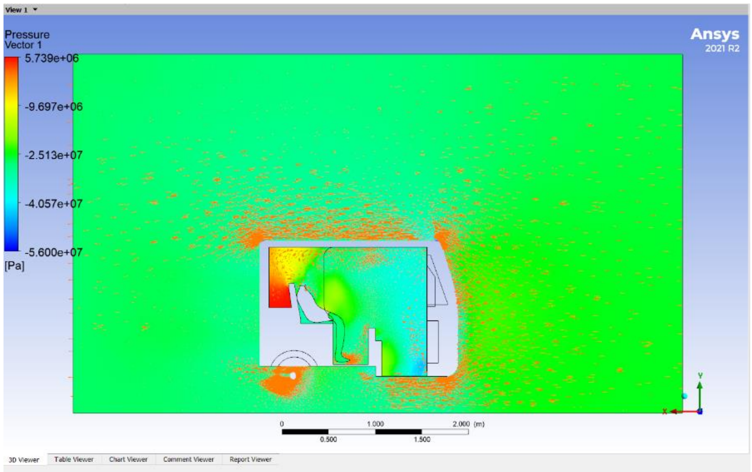

Figure 5.5: Pressure vector for vehicle without wind deflector

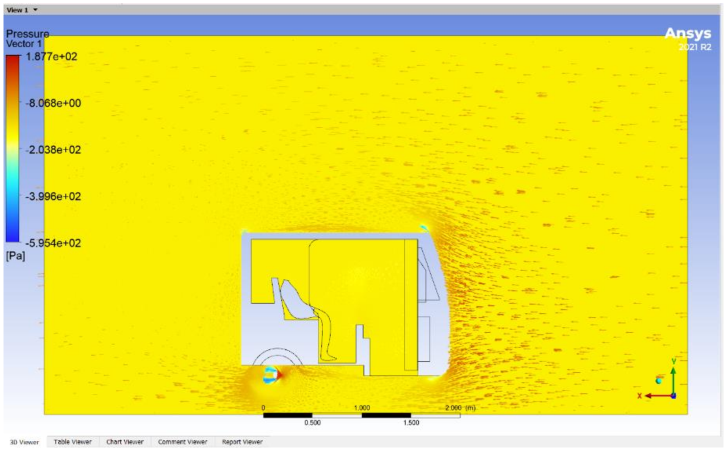

Figure 5.6: Pressure vector for vehicle with wind deflector of (width=15cm, θ=30)

From Figure 5.5 we can see the following results:

- High Pressure at the Back of the Passenger Seat: In this figure, the air that enters the vehicle gets trapped at the back of the passenger seat due to the lack of a clear passage for airflow. As the air is obstructed and cannot move freely, it starts to reverse direction and builds up, creating a high-pressure area. This is the zone where the maximum pressure concentration occurs inside the vehicle.

- Low Pressure at the Rear and Driver's Seat Areas: On the rear side of the vehicle and near the driver's seat, the pressure is at its lowest. This is because these areas experience a vacuum effect, where the airflow is not sufficiently replenished, leading to a pressure drop. The vacuum forms as air are unable to flow effectively through the vehicle's interior, resulting in a low-pressure region.

From Figure 5.6 we can see the following results:

- High Pressure at the Front, Top, and Bottom of the Vehicle: The highest pressure in this figure occurs on the external surfaces of the vehicle, particularly at the front, top, and bottom. This pressure is likely due to the aerodynamic interaction of the air with the vehicle's body, particularly in areas where the airflow is redirected by a wind deflector or similar design features.
- Low and Uniform Pressure inside the Vehicle: Inside the vehicle, the pressure distribution is more uniform and at a lower value compared to the scenario in Figure 5.5. The uniformity in pressure indicates that the introduction of a wind deflector or other modifications has helped to reduce the disruption of airflow inside the cabin. As a result, the pressure is more evenly distributed, providing a more stable and comfortable environment for passengers.
- Pressure Reduction with Wind Deflectors: The reduction in pressure inside the vehicle, especially when compared to vehicles without wind deflectors, is significant. Wind deflectors help guide airflow around the vehicle and prevent the creation of high-pressure zones inside, as seen in Figure 5.6. The deflectors thus improve the aerodynamic performance and comfort inside the vehicle by lowering internal wind pressure.

In Summary: Figure 5.5 shows a vehicle with significant pressure buildup at the back of the passenger seat due to airflow stagnation and reverse flow. This leads to higher internal pressures in some regions, while the rear and driver's seat areas experience a vacuum effect with low pressure. Figure 5.6 shows the impact of aerodynamic modifications (such as wind deflectors), where the pressure inside the vehicle is more uniform and lower. The external surfaces of the vehicle, especially at the front, top, and bottom, experience higher pressures, but the internal pressure is reduced compared to the scenario in Figure 5.5. This illustrates the positive effect of wind deflectors on reducing the pressure inside the vehicle compared to a vehicle without such modifications.

5.3 Validation

To validate the aerodynamic analysis results, a comparison was made between the drag coefficient obtained from the analysis and the value provided in the manufacturer's specifications for the Re 4S Bajaj. Figure 5.7 shows the technical specification of Bajaj RE three-wheeler.

Table 2. Technical specification of the Bajaj RE three-wheeler.

Mass of the vehicle (curb weight + payload weight)	678 kg (348 + 330 kg)
Maximum speed	65 km/h
Tyre	4.00–8.6 PR
Rolling resistance coefficient, C_{rr}	0.015
Drag coefficient, C_d	0.44
Frontal area, A_d	2.09 m^2
Gradeability	19%
Dimension (L × W × H)	2635 mm × 1300 mm × 1710 mm

Figure 5.7: Technical specification of Bajaj RE three-wheeler

The manufacturer's specifications specify a drag coefficient of 0.44, while the analysis yields a drag coefficient of 0.49 for the vehicle without wind deflector. the difference between the two values can be attributed to factors such as the difficulty in accurately modeling the exact dimensions of the vehicle and the limitation of 400 iterations for the analysis. These modeling challenges and iteration constraints can result in slight deviations from the manufacturer's value, as achieving an exact match is difficult under these conditions.

To quantify the error, the percentage error is calculated using the following formula:

Percentage error = (theoretical value – experimental value

$$\text{percentage error} = \frac{(\text{theoretical value} - \text{experimental values}) * 100\%}{\text{experimental values}}$$

$$\text{percentage error} = \frac{(0.44 - 0.49) * 100\%}{0.49}$$

Percentage error = 10 %

Therefore, the percentage error between the manufacturer's value and the analysis result is approximately 10 %. This small error is considered acceptable, given the complexities of CAD modeling and the limitations of computational resources. The results from the analysis are valid and provide a reasonable approximation of the aerodynamic characteristics of the vehicle.

CHAPTER SIX

CONCLUSION AND RECOMENDATION

This thesis deals with the design and aerodynamic analysis of the side wind deflector for the RE4S Bajaj. The 3D CAD model of the RE 4S Bajaj is developed using CATIA V5 software, and then it's imported to ANSYS software for the CFD analysis of the model. The dimension of the 3D model is taken directly from the existing RE 4S Bajaj with the scale of 1:1. The size and deflection angle of the deflector are optimized using the response surface method (RSM), in which eight different combinations of deflector width and deflection angle are used in the computational fluid dynamics (CFD) analysis.

6.1 The summary of CFD results

- The result obtained from the analysis shows maximum (drag coefficient = 0.49, lift coefficient = 0.1, drag force = 170.49N, and lift force = 34.71N) for the vehicle without a wind deflector.
- Minimum (drag coefficient = 0.38, lift coefficient = 0.08, drag force = 141.86 N, and lift force=30.18N) for vehicles with a deflector angle of 30^0 and a deflector width of 15 cm.
- The drag force is reduced by **16.8%** and lift force is reduced by **13.14%**
- For a vehicle without a wind deflector, the fluid flow streamlines show that air flows from the inlet side is deflected by the frontal area of the vehicle, then it enters the inside of the vehicle, which results in the disturbance of airflow. Due to this the passengers inside the vehicle will face a high wind pressure inside the vehicles.
- The result for vehicles with a deflector angle of 30^0 and a deflector width of 15 cm shows that the air coming from the inlet side is deflected by the wind deflector; due to this, most of the fluid stream line escapes from entering inside the vehicle.
- The residual plot shows residuals with a value of 1e-3, which indicates convergence of the analysis.

Summary of Vehicle Model Selection

- **Deflector Angle (30°)**: The chosen deflector angle is 30°, which is likely designed to optimally redirect airflow around the vehicle, reducing the amount of air that directly enters the vehicle compartment. This angle helps to reduce turbulence and allows the air to flow more smoothly over the vehicle, enhancing aerodynamic efficiency.
- **Deflector Width (15 cm)**: The deflector width of 15 cm indicates a relatively compact size, sufficient to modify the airflow without being overly large, which might otherwise introduce drag. The width helps to ensure that most of the incoming air is directed around the vehicle, contributing to reduced turbulence and pressure inside.

Aerodynamic Performance

- **Minimum Drag Force (141.86 N)**: The drag **force** is the resistance encountered by the vehicle as it moves through the air. A drag force of 141.86 N is relatively low, which is beneficial for fuel efficiency and vehicle stability at higher speeds. The wind deflector helps in reducing the drag by redirecting airflow and decreasing the disturbance created by the vehicle's front surface.
- **Minimum Lift Force (30.18 N):** The lift force represents the upward force acting on the vehicle. A lift force of 30.18 N is low, which ensures that the vehicle maintains better contact with the road, improving stability and safety, especially at high speeds. The deflector helps in keeping the airflow more stable around the vehicle, thereby reducing unwanted lift.

Streamline and Pressure Reduction

- **Streamlines Behavior**: The streamlines of the selected vehicle model show that the air from the inlet side is effectively deflected by the wind deflector. The deflector redirects the airflow around the vehicle, preventing most of the air from entering the vehicle's interior.
- **Reduced Wind Pressure**: As a result of the deflected air, the wind pressure inside the vehicle compartment is reduced. This not only leads to a more comfortable environment for passengers but also minimizes **wind buffeting noise**. The reduced pressure means that less turbulent air is allowed into the vehicle, which lowers both noise and discomfort typically caused by high-velocity airflow inside the cabin.

Generally, the combination of a 30° deflector angle and a 15 cm deflector width in the selected vehicle model has proven to be effective in reducing both the drag and lift forces, while also improving passenger comfort by reducing wind pressure and buffeting noise inside the cabin. These aerodynamic improvements suggest a well-optimized design that strikes a balance between performance (low drag and lift) and comfort (reduced internal wind pressure and noise).

6.2 Recommendation

- The CFD analysis of this thesis is carried out with 400 iterations because when the number of iterations increases, it takes a long time to analyze a single model, and it also requires the latest computer. However, for obtaining more precise results, it is advisable to utilize a number of iterations exceeding 1000.
- This study focused exclusively on the design and aerodynamic analysis of the side wind deflector for the RE4S Bajaj. However, the scope of this thesis does not extend to the physical manufacturing or real-world testing of the wind deflector. Therefore, for future projects and improvements, it is strongly recommended to manufacture and test the side wind deflector for the RE4S Bajaj.
- Additionally, manufacturers should consider the feasibility of mass production of these wind deflectors and integrate them into the vehicle's design. By implementing such design changes on a larger scale, manufacturers can provide consumers with more fuel-efficient, stable, and comfortable vehicles, addressing key consumer concerns such as fuel economy and ride quality.

6.3 Scope of future research

The scope of future research in the field of vehicle aerodynamics, particularly for three-wheeled vehicles like the RE4S Bajaj, offers numerous avenues for further exploration and improvement. This research focuses on advancing aerodynamic analysis methodologies, refining output parameters, and implementing more effective optimization techniques. Below are the key areas of future research that could significantly enhance aerodynamic performance analysis and the accuracy of related output parameters:

- Expanded CFD Analysis with Higher Iteration Counts: To examine the effects of increasing the number of iterations on aerodynamic accuracy and its impact on predicting drag forces, fuel consumption, and vehicle stability.
- Incorporating Real-World Environmental Variables: To create a more dynamic CFD model that accounts for environmental variables such as wind gusts, terrain variations, and changes in vehicle speed.
- Real-World Testing and Data Collection: To bridge the gap between simulation and reality by conducting on-road testing to validate aerodynamic performance predictions.

REFERENCES

Bappa, M. (2015). Aerodynamic Simulation of Vehicle Bodywork Design. Https://doi.org/10.13140/RG.2.2.16171.46884

Buscariolo, F. F., Magazoni, F., Maruyama, F. K., Alves, J. C. L., Della Volpe, L. J., & Holl, A. F. (2016). Aerodynamic enablers review for automotive applications. SAE Technical Paper.

Deaton, L., Rao, M., & Shih, W. (2007). Root cause identification and methods of reducing rear window buffeting noise. SAE Technical Paper.

Dunai, L., Lengua, I., Peris Fajarnés, G., & Iglesias Ortiz-Quintana, M. (2015). The effect of buffeting noise in passenger cars. Proceedings of Meetings on Acoustics, 23(1).

Gillespie, P. A., Johnston, J. D., Loriga, M. A., McCaffrey, K. J. W., Walsh, J. J., & Watterson, J. (1999). Influence of layering on vein systematics in line samples. Geological Society, London, Special Publications, 155(1), 35–56.

Gonzàlez Casal, I. (2013). Aerodynamic analysis and improvement of a roof box car.

Lemaitre, G., Vartanian, C., Lambourg, C., & Boussard, P. (2015). A psychoacoustical study of wind buffeting noise. Applied Acoustics, 95, 1–12.

Moffat, J. (2016). Aerodynamic Vehicle Design and Analysis. Blackpool and the Fylde College.

Reddy, N. S., Dhanraj, B., & Annavajjula, S. K. (2022). Analysis and calculation of drag force on vehicle with and without deflector.

Regin A, F., Manimanoharan, M., Reddy, A. B., & Nigam, P. (2013). Aerodynamic analysis of cabriolet passenger car: A design approach.

Schuetz, T. C. (2015). Aerodynamics of road vehicles. Sae International.

SEIFFERT, U. (2005). Handbook of automotive engineering.

Wang, Y. S., Sui, L. N., Yin, Z. Y., Wang, X. L., Liu, N. N., & Guo, H. (2017). A hybrid prediction for wind buffeting noises of vehicle rear window based on LES-LAA method. Applied Mathematical Modelling, 47, 160–173.

Yang, Z., Liu, L., & Gu, Z. (2022). Numerical Analysis and Optimization of the Front Window Visor for Vehicle Wind Buffeting Noise Reduction Based on Zonal SAS k-ε Method. Applied Sciences, 12(14), 6906.

Wood, R.M. (2004) Impact of advanced aerodynamic technology on transportation energy consumption. SAE Technical Paper 2004-01- 1306

Krishnani, P. N. (2009) CFD study of drag reduction of a generic sport utility vehicle, Master's Thesis, Mechanical Engineering Department, California State University, Sacramento.

Yadav, D., Kulkarni, P.S. and Ghiya, S., 2017. Response Surface Methodology Based Optimization of Aerodynamic Package of a FSAE Car. In Proceedings of the 19th Annual CFD Symposium. Bangalore, India: National Aerospace Laboratories.

Krajnovic, Sinisa. (2007) Aerodynamic optimization of vehicles using computational fluid dynamics and response surface methodology, In Proceedings of the XXI International Automotive Conference science & motor vehicles, pp. 1-11.

Lee, S.W. (2018). Computational analysis of air jet wheel deflector for aerodynamic drag reduction of road vehicle. Microsystem Technologies, 1–11.

Mukut, ANM Mominul Islam, and Mohammad Zoynal Abedin. (2019) Review on aerodynamic drag reduction of vehicles, International Journal of Engineering Materials and Manufacture 4, 1-14.

Hassan, SM Rakibul, Toukir Islam, Mohammad Ali, and Md Quamrul Islam. (2014) Numerical study on aerodynamic drag reduction of racing cars, Procedia Engineering 90. 308-313.

Wang, Qiliang, Xin Chen, and Yingchao Zhang. (2021) An overview of automotive wind noise and buffeting active control, SAE International Journal of Vehicle Dynamics, Stability, and NVH 5, no 10-05-04-0030, 443-458.

Bettes, WH. (1982) The Aerodynamic Drag of Road Vehicles – Past, Present and Future, Engineering & Science, 4-10.

Hoque, Ahmed Zawad Ul, Mohammad Ariful Islam, and Md Ahatashamul Haque Khan Shuvo. Aerodynamic Shape Optimization of Vehicles Using CFD Simulation.

Nath, D.S. et al. (2021) ‘Drag Reduction by Application of Aerodynamic Devices in A Race Car’, Advances in Aerodynamics, 3(1), p. 4.

Hariram, A. et al. (2021) ‘A Study in Options to Improve Aerodynamic Profile of Heavy-Duty Vehicles in Europe’, Sustainability, 11(19), p. 5519.

Fikri, Agus, Riyan Ariyansah, Firman Noor Hasan, Oktarina Heriyani, and Muhammad Ghiffar Sistani. (2024) Evaluating Wind Deflector Effect on Cargo Vans Aerodynamic Drag Using Computational Fluid Dynamics, Jurnal Asiimetrik: Jurnal Ilmiah Rekayasa & Inovasi, 211-220.

Ariyansah, R. (2019) ‘Modifikasi Desain Chasis Kendaraan Hybrid Pada Bus Scania K360LB’, Teknobiz : Jurnal Ilmiah Program Studi Magister Teknik Mesin, 7(3), pp. 156–165.

Gamayel, A. and Octavianus, G. (2021) Tutorial Ansys Workbench untuk Bidang Mekanikal. 2nd edn. Bandung, Indonesia: Media Sains Indonesia. [Print].

Li, Y. et al. (2023) ‘A Review on Numerical Simulation Based on CFD Technology of Aerodynamic Characteristics of Straight-Bladed Vertical Axis Wind Turbines’, Energy Reports, 9, pp. 4360–4379.

Djimtoingar, Solal Stephanie, Nana Sarfo Agyemang Derkyi, Francis Atta Kuranchie, and Joseph Kusi Yankyera.(2022) A review of response surface methodology for biogas process optimization, Cogent Engineering 9, no. 1: 2115283.

Davis, Mike. Buda's Wagon (2017) A brief history of the car bomb,Verso Books.

Satyanarayana, G., Ch Varun, and S. S. Naidu. (2013) CFD analysis of convergent-divergent nozzle. Acta Technica Corviniensis-Bulletin of Engineering 6, no. 3: 139.

Johnson, F. T., D. S. Kamenetskiy, R. G. Melvin, V. Venkatakrishnan, Laurence B. Wigton, D. P. Young, S. R. Allmaras, J. E. Bussoletti, and C. L. Hilmes (2011) Observations regarding algorithms required for robust CFD codes, Mathematical Modelling of Natural Phenomena 6, no. 3: 2-27.

Dhurve, Ms Arti Ramrao 2022-23) A Project Report on." PhD diss., Rashtrasant Tukadoji Maharaj Nagpur University.

https://en.wikipedia.org/wiki/Auto_rickshaw

https://simple.wikipedia.org/wiki/Auto_rickshaw

https://www.thereporterethiopia.com/31084/

https://www.automotiveworld.com/news-releases/lightyear-0-proven-the-most-aerodynamic-production-car-in-the-world/

APPENDIX

APPENDIX A

Overall Dimension of CAD Drawing

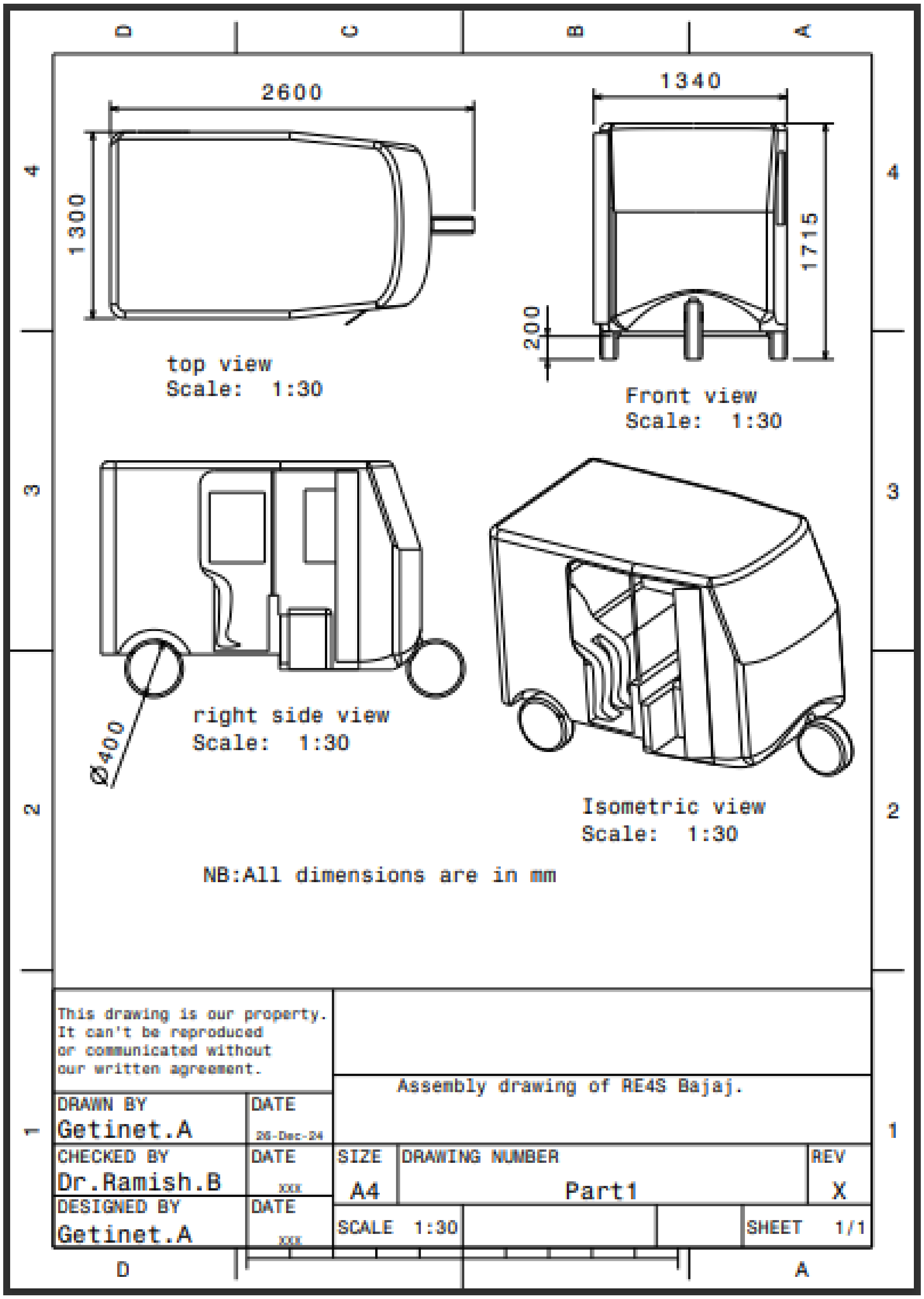

Figure A1: Overall dimension of CAD Drawing

APPENDIX B

3D model of the vehicle with wind deflector

Figure B1: 3D model of the vehicle with wind deflector

APPENDIX C

Iso surface or plane for velocity and pressure vector

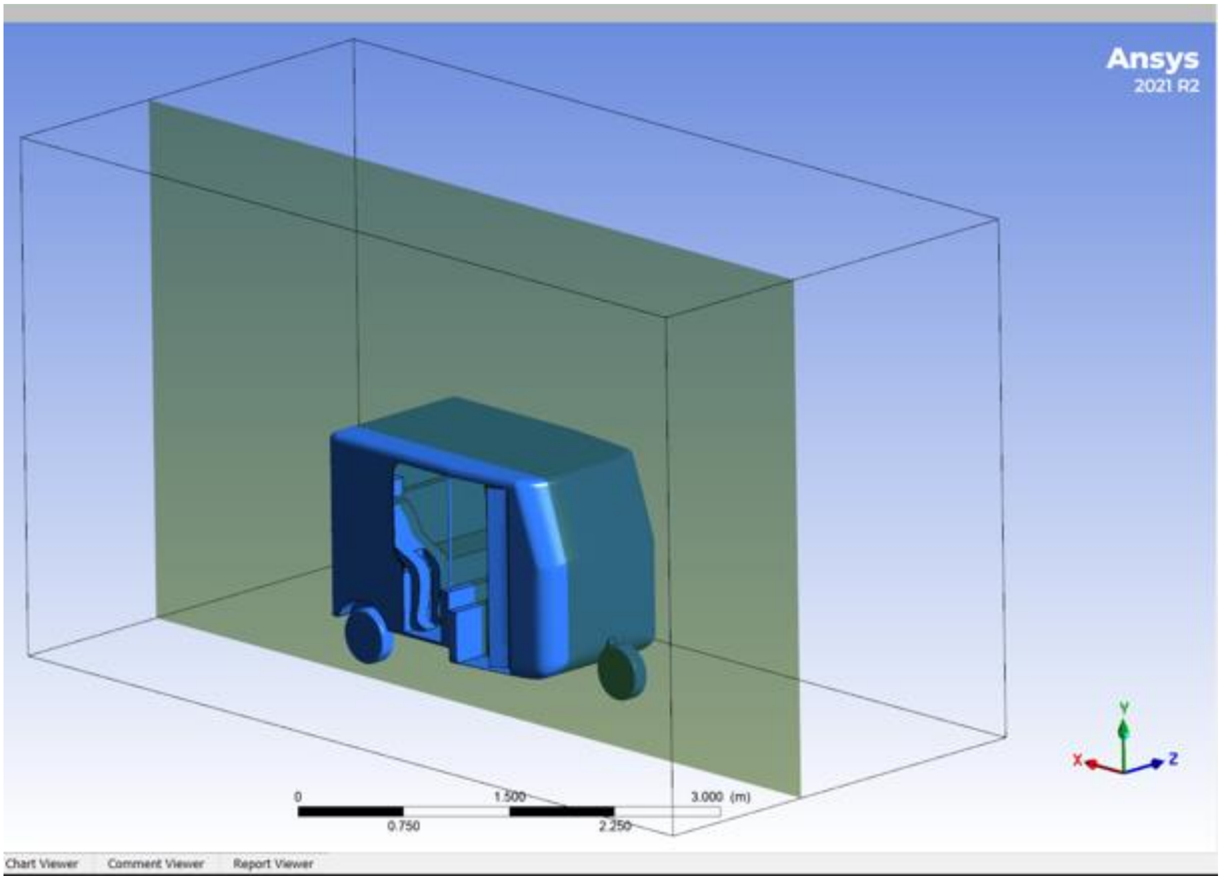

Figure C1: Iso surface for velocity and pressure vector

APPENDIX D

Meshing Of Vehicle Model with high quality meshing.

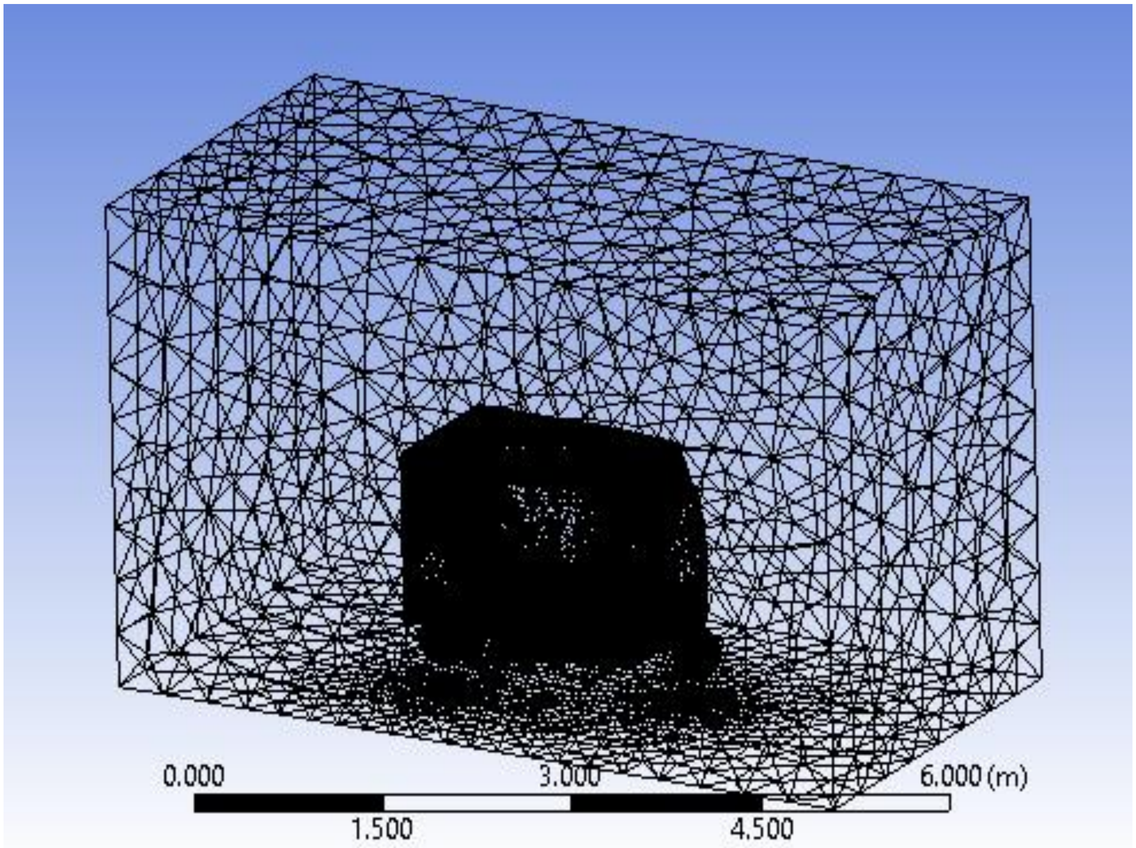

Figure D1: Meshing of Vehicle Model

APPENDIX E

Technical Specification of RE 4S Bajaj

Technical Specifications:

ENGINE

Type	Four stroke, Forced cooled SI.
Cubic Capacity	198.88 cc
Max power	7.6 kw at 5000 rpm
Max torque	17.0 Nm at 3500
Max Speed	65 kmph
Bore X Stroke-CM	63.5 mm X 62.8 mm
Transmission	Constant mesh, Manually operated 4 forward & 1 reverse
Clutch	Wet Multi-Disc Clutch

VEHICLE

Body	Monocoque chassis with central beam and welded cross member
Wheel Base	2000 mm
Length X Width X Height	2635X1300X1700 mm
Ground Clearance	200 mm - unladen
Turning Radius	2.88 m
Suspension Front	Offset Column with hydraulic shock absorbers and helical springs
Kerb Weight	348 kg
GVW	658 kg
Fuel Tank	8 L
Suspension Rear	Independently sprung rear wheels by trailing arms with helical springs and hydraulic shock absorbers

BRAKES & TYRES

Tyre Front	4.00-8,4 PR / 6PR
Tyre Rear	4.00-8,4 PR / 6PR
Brake Type Front	Drum
Brake Type Rear	Drum

ELECTRICALS

System	12 Volts DC -ve earth
Battery	12V, 32 AH
Horn	12V, Low Tone (LT)
Tail Lamps	12 V, 21W
Reserve Lamp	12 V, 10W
Wiper Motor	Single speed, Rated voltage 12 Volts
Head Lamps	12 35/35W

BAJAJ LOVED IN 70 COUNTRIES

BAJAJ RE The World's No.1 3-Wheeler

Figure E1: Technical Specification of RE 4S Bajaj